Journal of
Molluscan Studies

The Malacological Society of London

*Journal of Molluscan Studies* (2014) **80**: 585–603. doi:10.1093/mollus/eyu067
Advance Access publication date: 24 September 2014

A Special Issue of selected papers from the symposium: 'There's Something About Opisthobranchia', World Congress of Malacology, Ponta Delgada, Azores, July 2013

# 3D-microanatomy of the straight-shelled pteropod *Creseis clava* (Gastropoda: Heterobranchia: Euthecosomata)

R. A. Kubilius[1,2], P. Kohnert[1,2], B. Brenzinger[1,2] and M. Schrödl[1,2]

[1]*SNSB Bavarian State Collection of Zoology, Section Mollusca, Münchhausenstr. 21, 81247 Munich, Germany; and*
[2]*Department Biologie II, Biozentrum, Ludwig Maximilians–Universität, Großhaderner Str. 2, 82152 Planegg–Martinsried, Germany*

*Correspondence: P. Kohnert; e-mail: petekohnert@gmail.com*

(Received 5 February 2014; accepted 10 July 2014)

## ABSTRACT

The Thecosomata are pelagic euopisthobranch pteropods that are important for marine food chains, but threatened by ocean acidification. Members of the suborder Euthecosomata are either torted snails with a coiled, sinistral shell (Limacinidae) or are straight-shelled with a symmetrical body and an unusual ventral mantle cavity (Orthoconcha). The classification and taxonomy of euthecosomes still depends on shells, but is being challenged by initial molecular data. There is a large body of morpho-anatomical information dating from the beginning of the last century, and only biological (rather than soft-part anatomical) detail has been added since. For our initial study on pteropod morphoanatomy we have selected the potentially basal orthoconch genus *Creseis* Rang, 1828. Supplementing Meisenheimer's (1905) monographic work, we redescribe the microanatomy of the Mediterranean *C. clava* (Rang, 1828) from serial semithin sections and present 3D-models of all major organ systems. In the absence of histological differences we interpret the head to be fused with the foot, forming the wings with reduced labial tentacles and rhinophores. The postpharyngeal nerve ring is strongly condensed, showing fused buccal ganglia and a short visceral loop with two discernable ganglia. The genital system is monaulic and hermaphroditic, with female glands and a potential allosperm receptacle of unclear homology. An open seminal groove connects with the frontal copulatory organ, which shows complex penial infoldings. We confirm the 180° longitudinal rotation of the visceral organs relative to the condition in limacinids. As an alternative to ontogenetic detorsion, progenesis may have skipped torsion. Other obvious paedomorphoses such as single, basally forked tentacular nerves, suggest that heterochrony has been a driving force in thecosome evolution. Retaining the mantle cavity in a ventral position, *Creseis* has its large mantle gland—necessary for creating a mucus web for feeding—close to the mouth. Further comparative microanatomical data on orthoconchs and limacinids are needed to corroborate our assumptions of homology, and for reconstructing pteropod evolution once reliable molecular phylogenetic hypotheses are available.

## INTRODUCTION

The Pteropoda are the largest taxon of holopelagic gastropods and constitute a significant part of the marine zooplankton (Klussmann-Kolb & Dinapoli, 2006). As part of the euopisthobranch heterobranchs (Jörger *et al.*, 2010; Wägele *et al.*, 2014), pteropods are closely related to cephalaspidean snails and slugs, and are usually recovered as sister to sea hares (Anaspidea) in molecular phylogenetic analyses (Klussmann-Kolb & Dinapoli, 2006; Malaquias *et al.*, 2009; Göbbeler & Klussmann-Kolb, 2011). The Pteropoda contain two traditional opisthobranch orders, the shell-less Gymnosomata (estimated 40 species) and the Thecosomata. Since Meisenheimer's (1905) fundamental monographic work, Thecosomata have been divided into two suborders: the Pseudothecosomata with 23 valid species and a reduced or absent shell, and the Euthecosomata with at least 60 shelled species (current classification according to WoRMS, 2014). Euthecosomes represent an important food source for

other zooplankton including Gymnosomata, and for higher predators, such as fishes, birds and whales (Hunt *et al.*, 2008; Comeau *et al.*, 2010), and are an essential component in the marine carbon cycle (Feely *et al.*, 2004). As a consequence of their aragonitic shells ($CaCO_3$), euthecosomes are sensitive to the rising acidity of global seas (Feely *et al.*, 2004; Orr *et al.*, 2005; Comeau *et al.*, 2010). Euthecosomes are thus important and threatened members of marine ecosystems, as well as suitable study organisms for monitoring and predicting oceanic changes (Feely *et al.*, 2004; Bednaršek *et al.*, 2014).

In sharp contrast to their ecological relevance and the increasing amount of experimental work done on their physiology and resilience to environmental stress (Comeau *et al.*, 2012; Lischka & Riebesell, 2012), there has been little modern advance regarding pteropod morphology. Most of what is known of the external and internal anatomy and organ functions originated from early monographic works, such as those of Gegenbaur (1855) and Meisenheimer (1905). While several works (van der Spoel, 1967; Rampal, 1973, 2002, 2011; Lalli & Gilmer, 1989) added information on external features and functions (Lalli, 1970a, b; Lalli & Wells, 1978), soft-part anatomy basically remained unstudied. With sea slugs and other molluscs, modern 3D-micronatomical methodology has been shown to provide detailed and accurate data (e.g. Brenzinger *et al.*, 2011a; Brenzinger, Wilson & Schrödl, 2011b; Kohnert *et al.*, 2013; Brenzinger, Padula & Schrödl, 2013a; Brenzinger, Haszprunar & Schrödl, 2013b). Software-aided reconstruction of serial semithin histological sections is a highly suitable tool to assess, correct and supplement outdated, gross-morphological or paraffin-histology based knowledge (DaCosta *et al.*, 2007; Neusser & Schrödl, 2007; Neusser, Martynov & Schrödl, 2009).

For the first time in pteropods, we here aim to present 3D-anatomical models of a representative of the shelled thecosomes, the needle-shelled *Creseis clava* (Rang, 1828). According to the recent molecular phylogenetic hypotheses of Corse *et al.* (2013), the genus *Creseis* Rang, 1828 represents one of the earliest offshoots of all the straight-shelled euthecosomes, the Orthoconcha. The taxonomy of the family Creseidae has recently been reviewed by Gasca & Janssen (2014). The family is characterized by a bilaterally symmetrical, straight and pointed shell (Lalli & Gilmer, 1989), with a round aperture. The Creseidae currently comprise three genera and six species (Gasca & Janssen, 2014). *Creseis clava* is considered to be a senior synonym of the frequently used name *C. acicula* (Rang, 1828). Comparison of *C. clava* microanatomy with that of supposedly plesiomorphically coil-shelled euthecosomes such as *Limacina* may help to assess old hypotheses on the evolutionary emergence of the Orthoconcha associated with the decoiling of their shell, as assumed by Boas (1886).

## MATERIAL AND METHODS

Specimens of *Creseis clava* used in this study were collected using a plankton net towed vertically in open water near Fetovaia Bay (Elba, Italy) in June 1998. Specimens were preserved in 96% ethanol. For microanatomical examination and histology, specimens were decalcified using Bouin's fluid, dehydrated in a graded acetone series and submerged overnight in a 1 : 1 solution of Epon epoxy resin and 100% acetone. Fully infiltrated specimens were then embedded in pure Epon and set to polymerize for 1 d at 70 °C. One specimen block (ZSM Mol 20000023/1; Fig. 1) was trimmed manually with a razorblade, and serially sectioned (1.5 μm) using a diamond knife (Diatome Histo Jumbo) installed on a rotation microtome (Microm HM 360, Zeiss). Ribbons of serial sections were obtained by applying contact cement (Pattex Gel compact, Henkel) to the side of the specimen block facing the knife (Ruthensteiner, 2008). The ribbons were transferred to cleaned microscopy slides and stained with methylene blue/azure II stain following Richardson, Jarett & Finke (1960). Basophilic and osmiophilic structures stain blue, and metachromatic structures stain violet. Slides were then sealed with araldite resin (Romeis, 1989) and coverslips.

**Figure 1.** Examined specimen of *Creseis clava* embedded in Epon resin. Scale bar = 600 μm.

Sections were photographed using a Leica DMRD microscope with a Jenoptik ProgRes C3 digital camera and ProgRes CapturePro v. 2.8.0 software installed (Jenoptik, Jena, Germany). Every fourth image was used for 3D-reconstruction (of a total of 2,464 sections). After editing in Adobe Photoshop CS2 (Adobe Systems Inc.) software (resolution −50%, conversion to 8-bit grayscale, adjustments of contrast, brightness and sharpness) and XnView software (Kolor) (stack renaming), this resulted in a final image stack of 616 images with a resolution of 1,040 × 771 pixels (complete animal). An additional photo series of the same sections, but focusing on the central nervous system (CNS) and the penis, was created separately (477 sections with no gaps along the *z*-axis, imaged at higher magnification) using the same protocol. For 3D-reconstruction, image stacks were imported into Amira v. 5.4.3 software (Visualization Science Group, Mérignac, France) and processed according to the procedures described by Neusser *et al.* (2006) and Ruthensteiner (2008). Automatic alignment of images was carefully checked by hand; voxel size was calculated after measuring a selected area on a physical section in the microscope and applying the rule of three. In the aligned image stacks, anatomical structures were labelled manually (using 'brush' and 'lasso' tools); interpolation between sections was used where applicable. From these labels, rendered surface models were created; these are shown in Figures 2, 3, 6, 9 and 12. For histological figures, photographs were taken from the same sections.

## RESULTS

### *General morphology*

Body length of preserved *Creseis clava* specimen 3.6 mm. Body with short yet wide anterior headfoot complex and elongated, straight, conical and narrowly pointed posterior visceral mass (length 2.7 mm, maximal width 400 μm) (Fig. 2). These two body regions separated internally from each other by a muscular diaphragm. Headfoot complex partly retracted into visceral sac. Smooth transition between frontal, median cephalic lobe and lateral wings, i.e. no externally demarcated head. No rhinophores, labial tentacles or eyes detectable. Two flat and widespread wings attached to head anterolaterally, ventrally uniting in a small, median footlobe. Wingspan *c.*1.1 mm. Conspicuously ciliated field between mouth opening and median lobe, extending to half length of the wings on their ventral side (Fig. 3B). Body cavity (haemocoel) of head contains anterior digestive tract

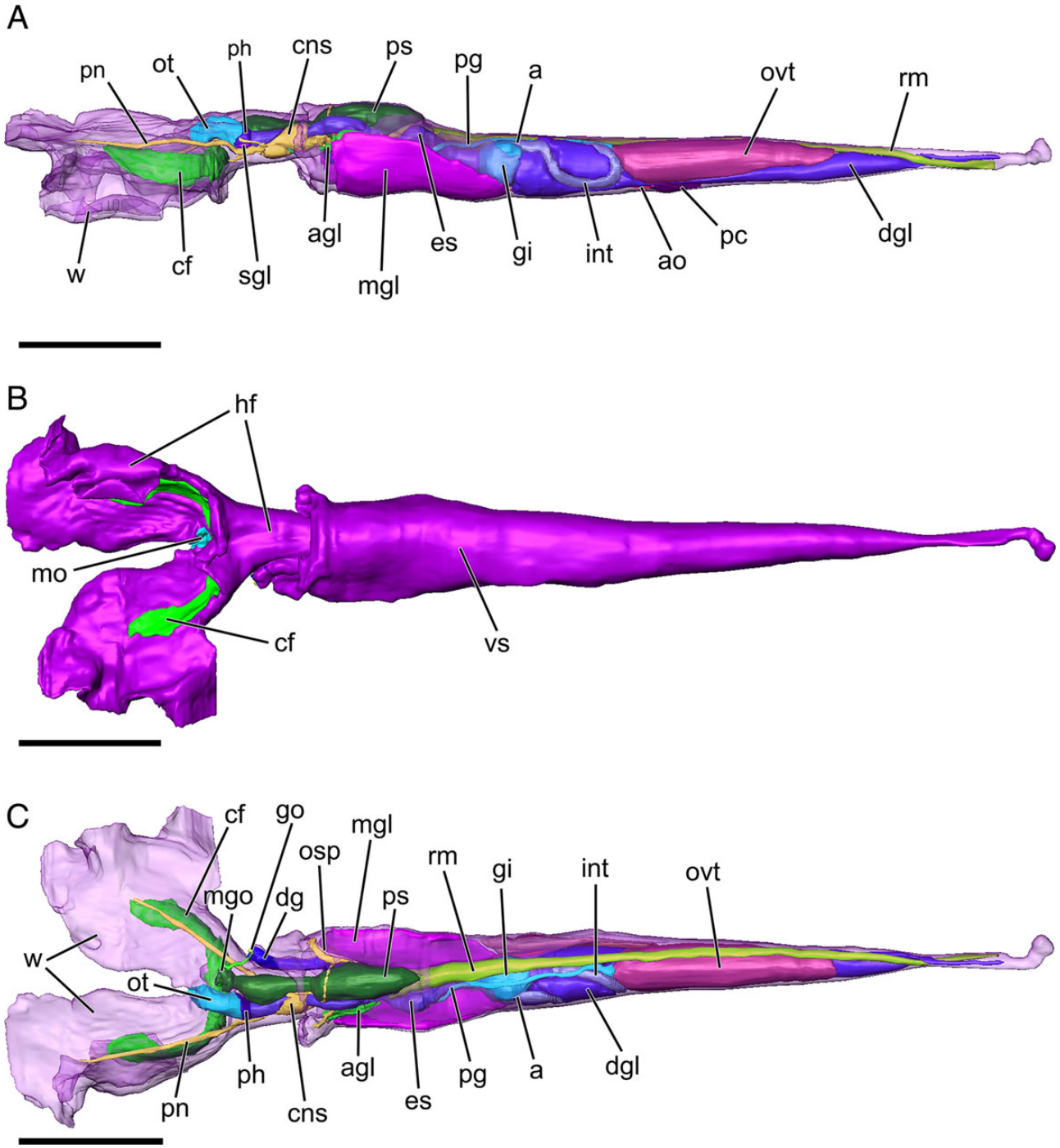


**Figure 2.** 3D-reconstructions showing the general morphology of *Creseis clava*. **A.** General organization of main organ systems, left lateral view. **B**. External morphology of examined specimen. **C.** General organization of the main organ systems, dorsal view. Abbreviations: a, anus; agl, anal gland; ao, aorta; cf, ciliary fields; cns, central nervous system; dg, distal gonoduct; dgl, digestive gland; es, oesophagus; go, genital opening; gi, gizzard; hf, headfoot complex; int, intestine; mgl, mantle gland; mgo, male genital opening; osp, osphradium; ot, oral tube; ovt, ovotestis; pc, pericard; pg, proximal gonoduct; ph, pharynx; pn, pedal nerve; rm, retractor muscle; ps, penial sheath; sgl, salivary gland; vs, visceral sac; w, wings. Scale bars = 500 μm.

(oral tube, pharynx, radula, salivary glands and oesophagus), CNS (postpharyngeal) and penis (Fig. 2A, C). Oesophagus penetrates diaphragm into visceral mass. Viscera enveloped by mantle. Mantle cavity situated ventrally, extending posteriorly below visceral sac for one-third of its length. Ventrally situated mantle 'roof' with large field of thick, glandular epithelium (mantle gland). Osphradium flat, elongated; situated anteroventrally, on right side of bottom of mantle cavity (Fig. 8F). Visceral sac contains posterior part of oesophagus, gizzard, stomach, caecum and intestine (Figs 4, 5). Reproductive system composed of posteriorly situated, large ovotestis (Fig. 2A, C), connected via gonoduct with complex of genital glands situated medially in anterior part of visceral sac. Genital glands connected to genital opening on right side of mantle cavity, in foremost part of visceral sac (Fig. 9A). Kidney located on right side of visceral sac, forming excretory and circulatory systems together with heart and

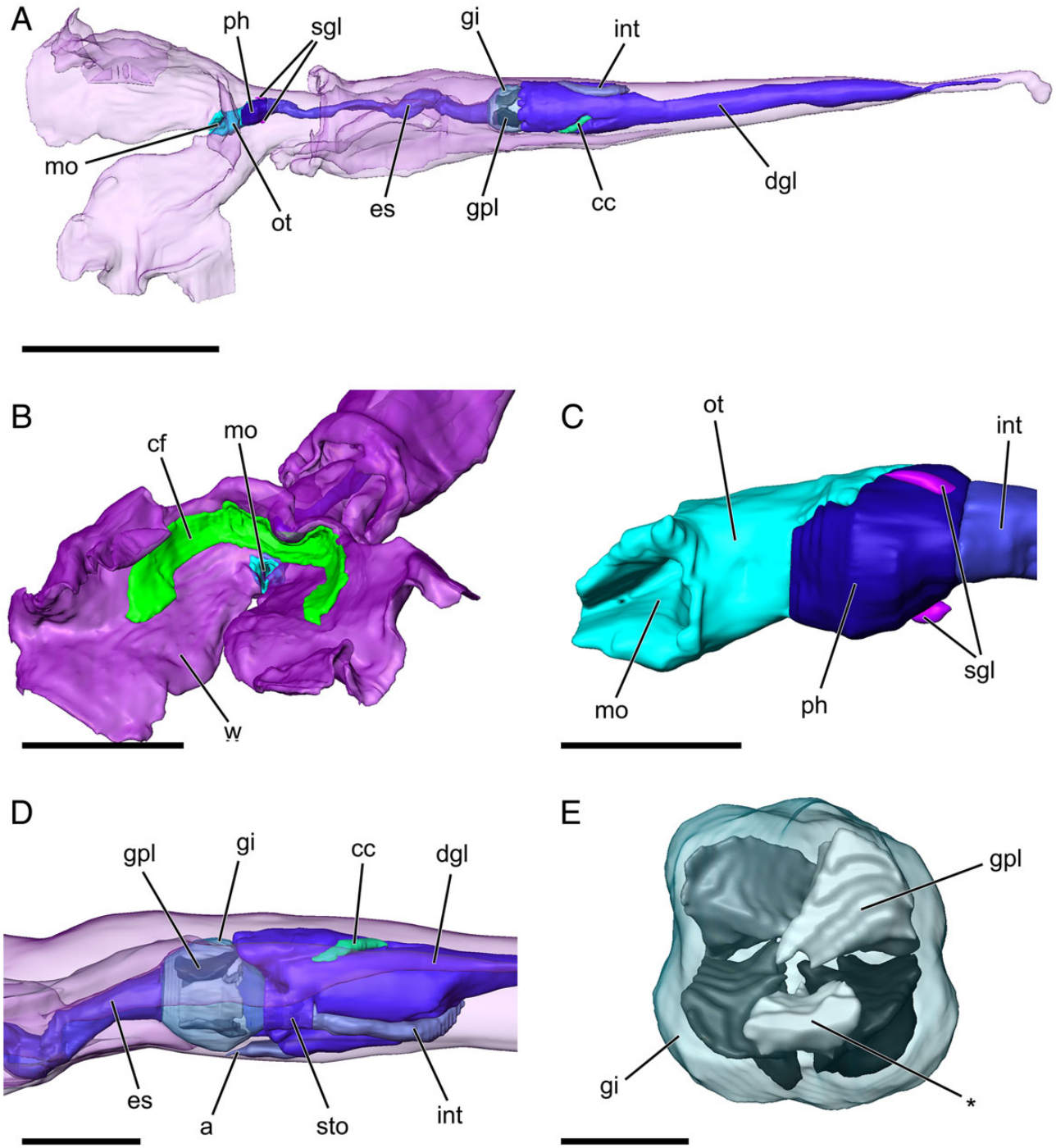


**Figure 3.** 3D-reconstruction of the digestive system of *Creseis clava*. **A.** Overview of digestive system within the specimen, ventrolateral view. **B.** Ciliary fields and mouth opening, anteroventral view. **C.** Ventral view of pharynx and associated organs. **D.** Arrangement of posterior digestive organs, dorsolateral view. **E.** Gizzard and gizzard plates, posterior view. Note smallest, 5th gizzard plate (*). Abbreviations: a, anus; cc, caecum; cf, ciliary field; dgl, digestive gland; es, oesophagus; gi, gizzard; gpl, gizzard plates; int, intestine; mo, mouth opening; ot, oral tube; ph, pharynx; sgl, salivary glands; sto, stomach; w, wings. Scale bars: **A** = 700 μm; **B** = 400 μm; **C** = 100 μm; **D** = 200 μm; **E** = 70 μm.

pericardium (Fig. 12). Kidney opens into anterior part of mantle cavity through nephropore on its left side (Fig. 13D).

*Mantle cavity organs*

Anterior mantle edge with mantle edge gland (= shell gland) forming a complete ring, consisting of glandular epidermal cells. Mantle cavity with two epidermal glands: large, outer mantle gland and smaller, inner anal gland. Mantle gland a flat, convex, very extensive organ (length 600 μm, width 350 μm), situated in anterior section of visceral sac (Fig. 2A, B), occupying entire inner epithelium of ventrally situated roof of mantle cavity. Mantle gland (= pallial gland) extending ventrally to envelop most of the anterior organs (Fig. 2A, B), such as penis sheath, female genital glands, oesophagus, osphradium gland. Mantle gland cells very large and

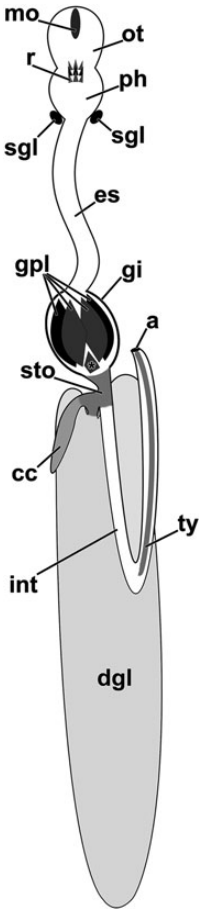


**Figure 4.** Schematic overview of the digestive system of *Creseis clava*, ventral view. Abbreviations: a, anus; cc, caecum; dgl, digestive gland; es, oesophagus; gi, gizzard; gpl, gizzard plates; int, intestine; mo, mouth opening; ot, oral tube; ph, pharynx; r, radula; sgl, salivary glands; sto, stomach; ty, typhlosolis. Note 5th gizzard plate (*). Connection of salivary glands to pharynx not detectable.

columnar, arranged around longitudinal axis of body, having granular cytoplasm with distinctive staining, showing transition from dark blue base to colourless apical areas. Anal gland of unclear homology; flat, 220 μm in length and 50 μm in width, situated on left side of mantle cavity, opposite to osphradium (Fig. 2A, C). Anal gland part of inner wall of mantle cavity, built up by single layer of cells, containing very large nuclei and many clear and unstained vesicles, orientated towards mantle cavity (Fig. 13E).

### *Retractor muscle*

A 2.13 mm long, roughly cylindrical muscle extends mediodorsally throughout length of visceral sac, from posteriormost part of visceral sac to posterior part of penis sheath (Figs. 9A and 13B). Structure straight, increasing in width anteriorly (posteriorly 15 μm, anteriorly 80 μm). 3D-model incomplete because of muscle being damaged in its most anterior part, showing indistinct ramification into two branches.

### *Digestive system*

Mouth opening located medioventrally between bases of wings. Oral tube short, thin-walled (Fig. 3A, B). Lumen of anterior part of oral tube round in cross section, roughly V-shaped approaching pharynx. Pharynx about 220 μm long, up to 120 μm wide, with thick muscular layer surrounding buccal lumen (Fig. 3C). Radula with nine teeth in three rows (radula formula 3 × 1.1.1) (Fig. 5A). Each row of one triangular median tooth and two hook-shaped lateral teeth. Two very short and small salivary glands lateral to pharynx; salivary ducts not detected. Tubular oesophagus 780 μm long, with ciliated epithelium multiply folded, lumen star-shaped in cross section (Fig. 5B.). Folding of oesophagus successively reduced towards its posterior end, with volume of lumen increasing. Gizzard short yet broad, voluminous, resembling a spherical bag. Gizzard with thick outer muscular layer; containing five almost unstained, chitinous, pyramidal gizzard plates. Gizzard plates attached basally to epithelium, with their peaks pointing towards centre of gizzard lumen. Four plates (length *c*.110 μm) form anterior ring of gizzard plates; 5th plate only 55 μm long, medioventral, slightly posterior to rest of plates (Figs 3D, E, 4, 5C). Posterior end of gizzard connected to stomach. Three different structures branch from stomach: digestive gland, caecum and intestine. Digestive gland large, lobed, 1.7 mm in length, 190 μm in maximal width, extending to most posterior part of visceral sac. Digestive gland of many peripheral lobes arranged densely around (central) main duct (Figs 3A, 5D–F). Lower density of branching lobes towards posterior end of digestive gland. Cells of digestive gland with granular cytoplasm. Caecum a blindly ending, small, elongate sac-like organ, ciliated, 120 μm long, 20 μm wide (Figs 4, 5D, E). Intestine *c*.800 μm long, densely ciliated tube leaving stomach posteriorly, looping around left anterior part of digestive gland. Loop turning at first ventrally to left side, then flipping backwards. Intestinal cells cylindrical, short. Distal third of intestine with distinct typhlosole (Figs. 4, 5F). Anus small, directed anteriorly, mediodorsal in visceral sac, directly above gizzard.

### *Central nervous system*

CNS in head cavity, consisting of postpharyngeal, circumesophageal nerve ring and posterior visceral loop. Visceral loop ganglia densely arranged, partly fused. Each ganglion with outer thick cortex of dark blue stained perikarya, and inner light blue stained medulla containing exclusively nerve fibres. Nerve ring of paired pedal and cerebropleural ganglia. Oval pedal ganglia (length 110 μm, width 60 μm) anterior to cerebropleural ganglia, lateroventral to oesophagus. Single pedal commissure short, thick (Fig. 8A). Two statocysts embedded on top of posterior end of pedal ganglia. Pedal ganglia connected with cerebropleural ganglia by two separate connectives each. Completely fused cerebropleural ganglia large (length 130 μm, width 100 μm), encompassing oesophagus laterally, with distinct dorsal commissure 50 μm long. Buccal ganglia elongated (length 78 μm, width 30 μm), fused medially, wedged between oesophagus, cerebropleural and pedal ganglia (Fig. 8B). Buccal-cerebropleural connectives short, thin.

Direct transition of cerebropleural ganglia into fused visceral loop ganglia, without any recognizable connectives. Visceral loop short (length 90 μm, width 130 μm), comprised of two almost completely fused ganglia. Ganglia nevertheless distinguishable by rudimentary inner separations through perikarya: one larger (fused suboesophageal and visceral ganglia) ganglion (length 90 μm, width 80 μm), situated on left side of visceral loop; one smaller (supraoesophageal) ganglion (length 75 μm, width 50 μm), situated on its right side.

Each pedal ganglion with strong pedal nerve (width 20 μm) emerging anterolaterally, progressing towards anterior part of head-foot, ramifying into at least three branches (Figs 6, 7). Pedal nerves innervating both wings with at least one of their branches; exact numbers of branches, trajectories and target areas not detectable.

A paired cerebral nerve (10 μm diameter) emerges anteriorly from each cerebropleural ganglion and progresses lateroventrally along each pedal ganglion towards buccal mass, ramifying

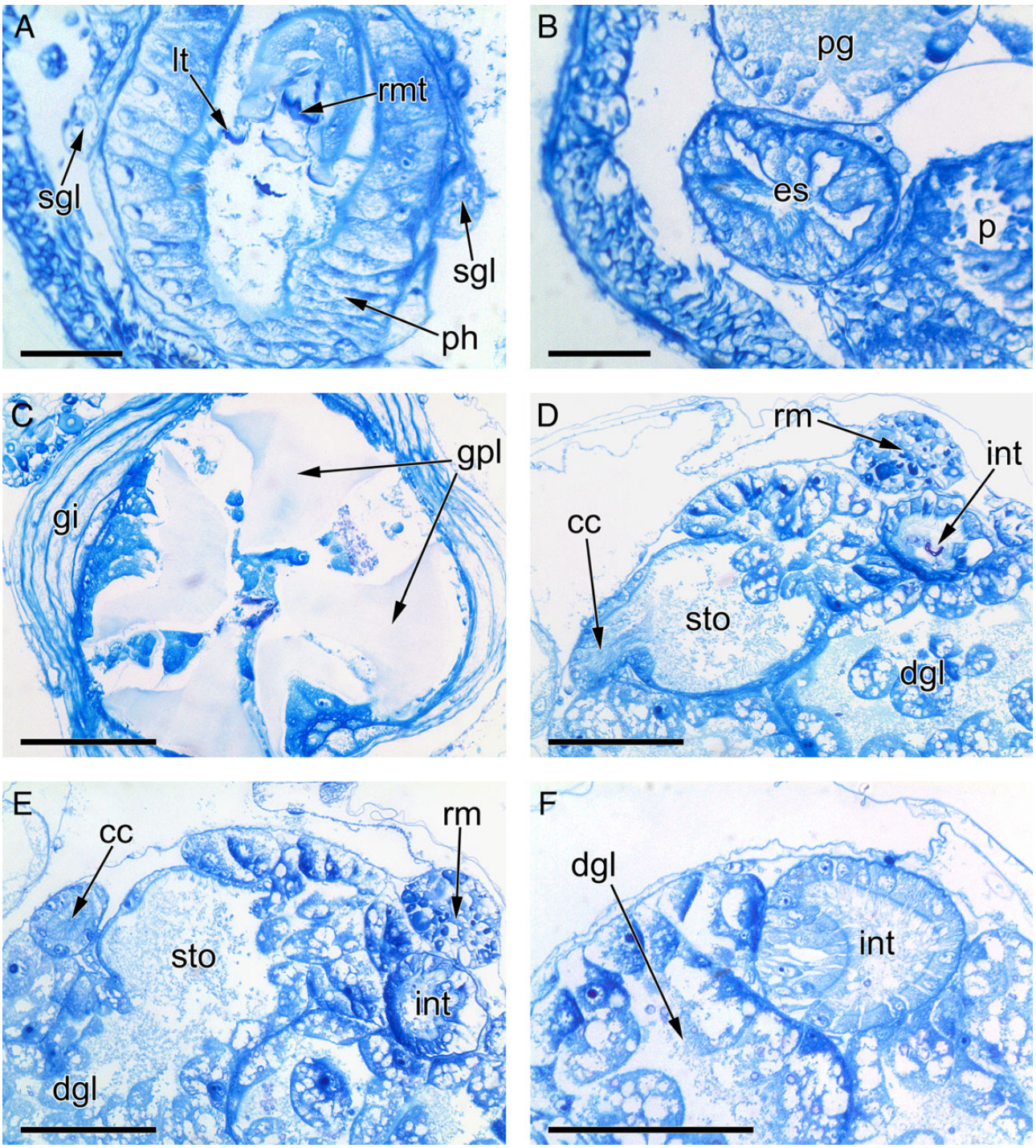


**Figure 5.** Semithin cross sections of the digestive system of *Creseis clava*. **A.** Pharynx. **B.** Oesophagus. **C.** Gizzard. **D.** Connection of stomach and caecum. **E.** Connection of stomach and digestive gland. **F.** Distal part of intestine. Abbreviations: cc, caecum; dgl, digestive gland; es, oesophagus; gi, gizzard; gpl, gizzard plates; int, intestine; lt, lateral tooth; pg, pedal ganglion; ph, pharynx; p, penis; rmt, radular median tooth; sgl, salivary gland; sto, stomach; rm, retractor muscle. Scale bars: **A**, **B** = 25 μm; **C**, **D**, **E**, **F** = 50 μm.

into two branches after about 100 μm. Branches of left nerve apparently innervating left side of pharynx; branches of right nerve enter right side of pharynx and anterior end of penis/penis sheath, respectively.

Fused buccal ganglia gives rise to two nerves, progressing laterally, alongside oesophagus towards buccal mass. Buccal nerves narrow (5–7 μm), without ramifications; innervating ipsilateral sides of pharynx (Figs 6C–F, 7).

Visceral loop ganglia with three distinctive nerves. Two nerves emerge from larger, left ganglion, one from smaller right ganglion. Left ganglion with delicate posterior nerve (5 μm diameter) proceeding alongside oesophagus into visceral sac; nerve convoluted, running multiple times back and forth. Second left ganglion nerve thick (15–20 μm), running for 60 μm towards posterior left part of head with U-turn shortly after penetration of diaphragm, thus progressing along

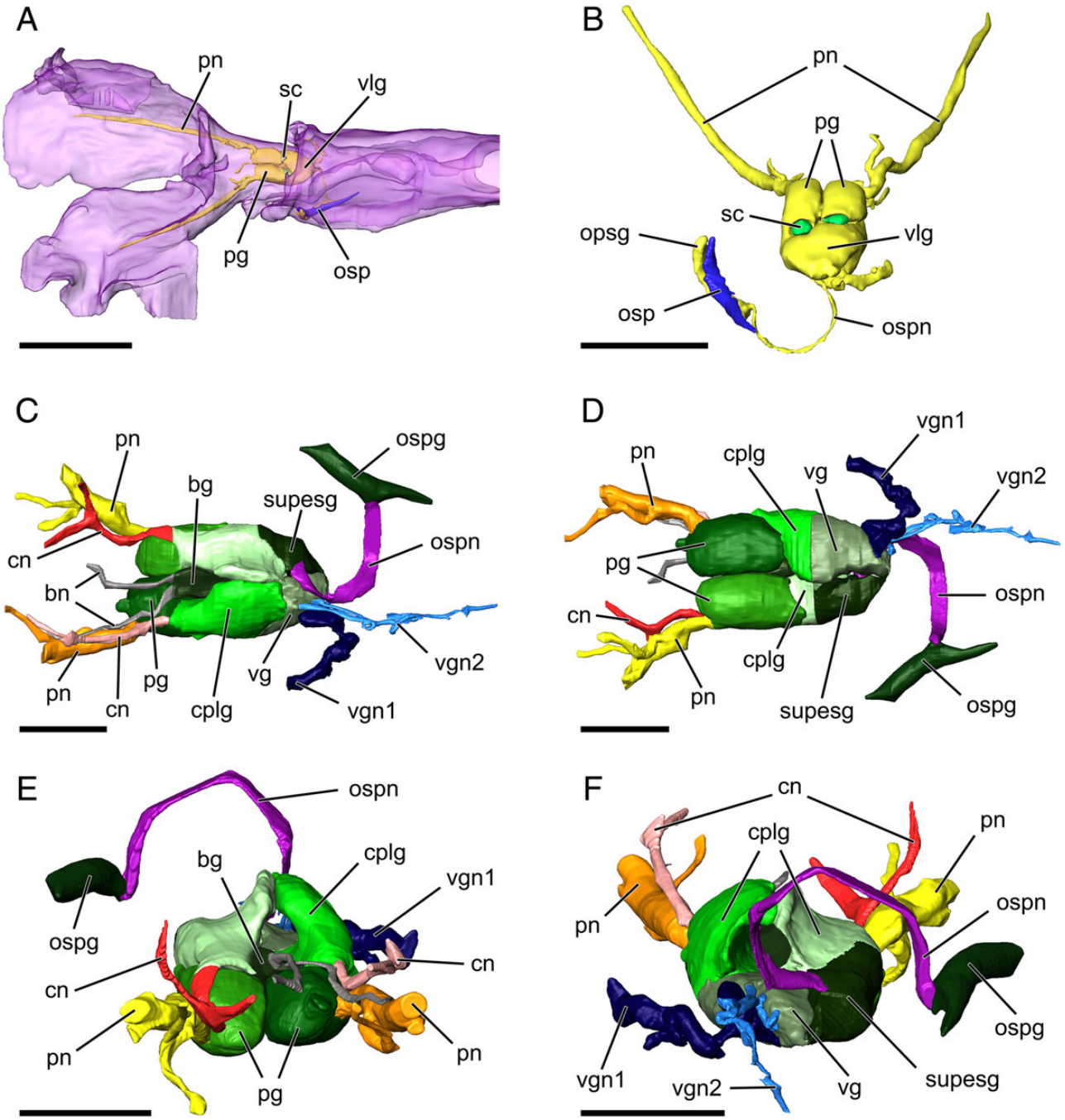


**Figure 6.** 3D-reconstruction of nervous system of *Creseis clava*. **A.** Localization of central nervous system (CNS) within specimen, ventral view. **B.** Posteroventral view of complete CNS. **C.** Complete CNS, dorsal view. **D.** Complete CNS, ventral view. **E.** Anterior view of complete CNS. **F.** Posterior view of complete CNS. Abbreviations: bg, completely fused buccal ganglion; bn, buccal nerve; cn, cerebral nerve; cplg, cerebropleural ganglion; opsg, osphradial ganglion; osp, osphradium; ospn, osphradial nerve; pg, pedal ganglion; pn, pedal nerve; sc, statocyst; supesg, supraoesophageal ganglion; vlg, visceral loop ganglia; vg, visceral ganglion; vgn1, visceral ganglion nerve 1; vgn2, visceral ganglion nerve 2. Scale bars: **A** = 400 μm; **B** = 200 μm; **C–F** = 100 μm.

left side of anterior part of mantle cavity wall (Figs 6C, D, F, 7); there apparently innervating mantle cavity gland. Right visceral loop ganglion with anterior, flattened nerve (width 20 μm, thickness 3–5 μm), running dorsally along and then around penis sheath, finally connecting to osphradial ganglion (length 230 μm, width 25 μm). Osphradial ganglion on right side of anterior part of visceral sac, directly below osphradium.

*Sensory organs*

Paired statocysts and unpaired osphradium. No traces of eyes. Two ellipsoid statocysts (50 μm long, 35 μm wide) ventral in head, between pedal and cerebropleural ganglia (Fig. 8C, E). Each statocyst with its anterior half embedded in respective pedal ganglion. Innervation of statocysts not recognized. Statocysts with thin outer wall of flattened cells with large nucleus; inner lumen, appearing empty in histological sections. Osphradium flat,

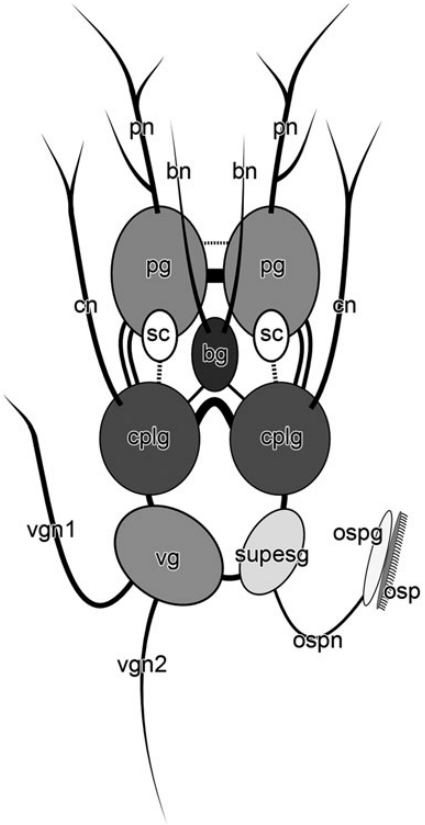


**Figure 7.** Schematic overview of CNS of *Creseis clava*, dorsal view. Dashed lines represent nerves that could not be identified in reconstructed specimen but were mentioned in the literature. Abbreviations: bg, buccal ganglion; bn, buccal nerve; cn, cerebral nerve; cplg, cerebropleural ganglion; osp, osphradium; ospg, osphradial ganglion; ospn, osphradial nerve; pg, pedal ganglion; pn, pedal nerve; sc, statocyst; vg, visceral ganglion; supesg, supraoesophageal ganglion; vgn1, visceral ganglion nerve 1; vgn2, visceral ganglion nerve 2.

elongated, on right of anterior part of visceral sac, of inconspicuously ciliated epithelium in outer wall of mantle cavity. Osphradial epithelium of single layer of cubic cells, with granular intracellular medium (Fig. 8F).

### *Genital system*

Reproductive system of *C. clava* (Figs 9–11) monaulic, with posterior organs located in visceral sac (ovotestis, three female genital glands) and anterior copulatory apparatus situated in head cavity (Fig. 9A, B).

*Palliovisceral genital components*: Massive elongated hermaphroditic gonad (length 780 μm; width 160 μm; Figs 9A, 11A) with peripheral layer of blue stained cells; fewer large cells (potential oocytes) with blue-staining cytoplasm and dark blue stained nucleus (Fig. 11A). Proximal gonoduct with small lumen; cilia not detectable. Gonoduct straight, connecting with three densely packed, but distinct, glandular organs (Figs 9, 10). This glandular complex (Figs 9C, 10, 11B) situated medially in anterior part of visceral sac beneath oesophagus, extending towards right lateral part of neck region (Fig. 9A). First genital gland smallest (gland 1; length 80 μm, width 50 μm). Gland 2 largest (length 360 μm, width 60 μm). Short sac-like gland 3 (length 140 μm, width 25 μm) connecting to both other glands. Histology of glands 1 and 2 (potential female glands) similar, both of round and cylindrical cells, with granular content stained dark to light blue (Fig. 11B, C). Cells of gland 2 with light pink stained granules in apical parts. Cells of gland 3 (potential allosperm receptacle) stout, containing granules stained light blue. Gland 2 narrowing distally into distal gonoduct, latter part with columnar epithelium (Fig. 11B). Distal gonoduct connecting to genital opening, on right side of most anterior part of mantle cavity (Figs 9A, D, 11D).

*Copulatory organ*: Epidermal sperm groove (130 μm long), without clearly detectable cilia, linking genital opening to male genital opening (Fig. 11D). Male copulatory organ (i.e. cephalic penis; length 720 μm, width 130 μm) completely enveloped by a sheath, extending into posterior part of head cavity. Epithelium of sheath invaginated with complex infoldings, with multiple irregular ramifications into large and voluminous caeca along its length (Figs 10, 11F); of large, very elongated, densely packed cells with mostly dark blue stained granular content. Caeca interconnected by narrow lumina (Fig. 11E); no spines or copulatory stylets detected.

### *Circulatory and excretory systems*

Monotocardian heart (Figs 12B, 13A) of thick-walled ventricle and thin-walled auricle. Heart medioventral, halfway through visceral sac, close to posterior end of kidney (Fig. 12A–C). Heart enveloped by flattened, thin pericardium (length 160 μm, width 100 μm). Thin-walled, flat, sac-like venous sinus penetrating pericardium on its right side (Fig. 12B), merging into auricle. Auricle (length 50 μm, width 30 μm) with many convolutions in its thin, light blue stained wall, extending through dark blue stained, thick wall of oval ventricle (length 60 μm, width 40 μm) on its right side (Fig. 13A). Aorta emerging from anterior end of ventricle, penetrating pericardium medially (Fig. 12B, C), progressing towards anterior part of visceral sac (Fig. 12A). Aorta (length 1.2 mm, width 8 μm) thin-walled, narrow, tubular (Fig. 13B), running through almost entire visceral sac, apparently opening into visceral cavity above left anterior-most edge of mantle gland, posterior to CNS.

Kidney (length 630 μm, width 90 μm) tubular (Fig. 12A), with slight dorsoventral depression, situated in middle third of visceral sac on its right side. Kidney with large lumen surrounded by single layer of large, flattened cells. These light blue stained cells with large nucleus and granules in cytoplasm (Fig. 13D). Posterior portion of kidney without visible lumen, with cells increasing in volume. Kidney connected with anteriorly situated pericardium via 10 μm long renopericardioduct (Figs 12B, 13C). Nephroduct emerging from anterior left part of kidney. Small nephropore opening into mantle cavity (Fig. 13D).

## DISCUSSION

This study is the first comprehensive anatomical account of an entire pteropod for over a century. Other previous studies were mostly based on gross dissections, or on only a few histological sections, or focused solely on particular organs or the shell (e.g. Fahrner & Haszprunar, 2000; Janssen, 2012). We here attempt to establish a dataset as a basis for future studies on *Creseis* and related taxa. The homology of pteropod features needs to be re-evaluated in the light of modern hypotheses on heterobranch phylogeny and evolution (Schrödl *et al.*, 2011; Wägele *et al.*, 2014). We compare our description of the microanatomy of *C. clava* with available descriptions, particularly those of Meisenheimer (1905). However, Meisenheimer presented a comparative account of thecosome anatomy rather than providing coherent descriptions of particular species.

### *External morphology*

The 3-D reconstruction of *C. clava* coincides in most respects with the general morphology of the Euthecosomata described

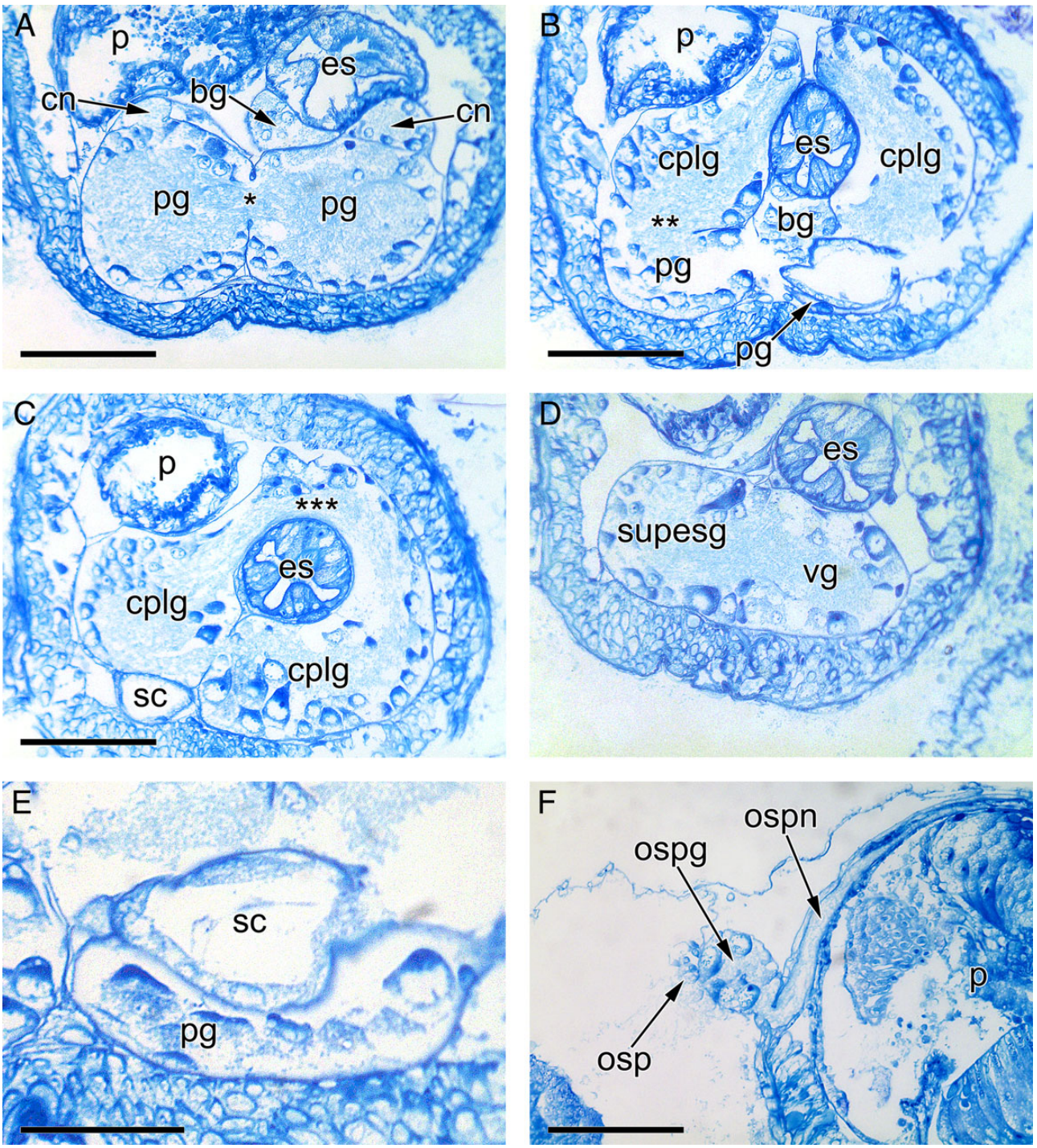


**Figure 8.** Semithin cross sections of nervous system of *Creseis clava*. **A.–C.** Arrangement of several ganglia of nerve ring. **A.** Cross section of pedal ganglia and surrounding organs. Note strong pedal commissure (*). **B.** Cross section of nerve ring showing cerebropedal commissure (**). **C.** Cross section of cerebropleural ganglia. Note extensive cerebral commissure (***). **D.** Cross section showing strong fusion of ganglia on visceral loop. **E.** Statocyst embedded in pedal ganglion tissue. **F.** Cross section of osphradial ganglion and osphradial nerve. Abbreviations: bg, buccal ganglion; cn, cerebral nerve; cplg, cerebropleural ganglion; es, oesophagus; osp, osphradium; ospg, osphradial ganglion; ospn, osphradial nerve; p, penis; pg, pedal ganglion; sc, statocyst; supesg, supraoesophageal ganglion; vg, visceral ganglion. Scale bars: **A–D, F** = 50 μm; **E** = 25 μm.

by Meisenheimer (1905). All thecosomes show the typical gastropod subdivision into an anterior headfoot complex and a posterior visceral sac.

The headfoot of pelagic Pteropoda, in particular euthecosomes, differs radically in external morphology from that of related euopisthobranchs. The latter plesiomorphically have a demarcated head with two pairs of head tentacles (Wägele & Klussmann-Kolb, 2005; Brenzinger *et al.*, 2013a), i.e. anterior labial tentacles and more posterior rhinophores, which are also present in sea hares, the putative sister group of pteropods. As is evident from our data, *C. clava* lacks a demarcated head and does not possess well-elaborated head appendages; there also are no unambiguously detectable eyes. Reports on other thecosomes have mentioned one pair of posterior tentacles, which could

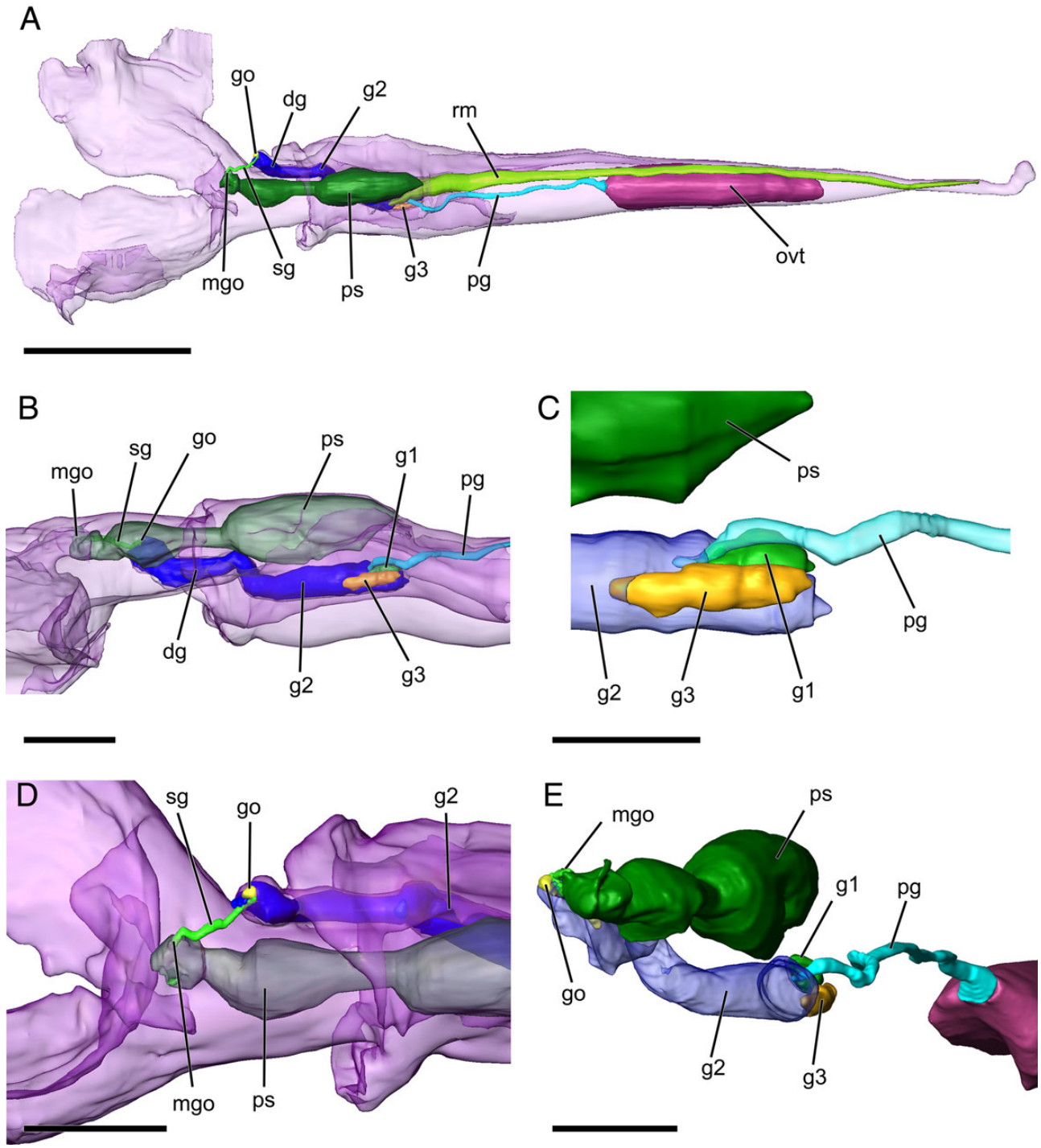


**Figure 9.** 3D-reconstruction of genital system of *Creseis clava*. **A.** Localization of genital system within examined specimen, dorsal view. **B.** Left lateral view of complex of genital glands and penial sheath. **C.** Complex of genital glands, left lateral view. **D.** Epidermal groove between genital openings (sperm groove), dorsal view. **E.** Anterolateral view of general genital arrangement. Abbreviations: dg, distal gonoduct; g1, genital accessory gland 1; g2, genital accessory gland 2; g3, genital accessory gland 3; go, genital opening; mgo, male genital opening; ovt, ovotestis; pg, proximal gonoduct; ps, penial sheath; rm, retractor muscle; sg, sperm groove. Scale bars: **A** = 600 μm; **B, D** = 200 μm; **C** = 100 μm; **E** = 150 μm.

represent homologues of rhinophores according to Corse *et al.* (2013). In thecosomes, the left rhinophore may be more or less reduced and the right one associated with a basal, more or less rudimentary eye. In contrast to our material, rudimentary tentacles (i.e. putative rhinophores) were indeed observed in some *Creseis* species (Gegenbaur, 1855; van der Spoel, 1967); Meisenheimer (1905) also mentioned a rudimentary, unpigmented eye for the genus.

Some thecosomes show small stubby tentacles along the anterior edge of their wings (Meisenheimer, 1905), often referred to as 'tentacle-like' structures (Corse *et al.*, 2013) or 'wing protrusions' (van der Spoel, 1967); these are visible in living specimens, but not evident from our preserved material. We interpret these tentacles as rudimentary labial tentacles, which are also present in the sister group Gymnosomata and most other, noninfaunal Euopisthobranchia.

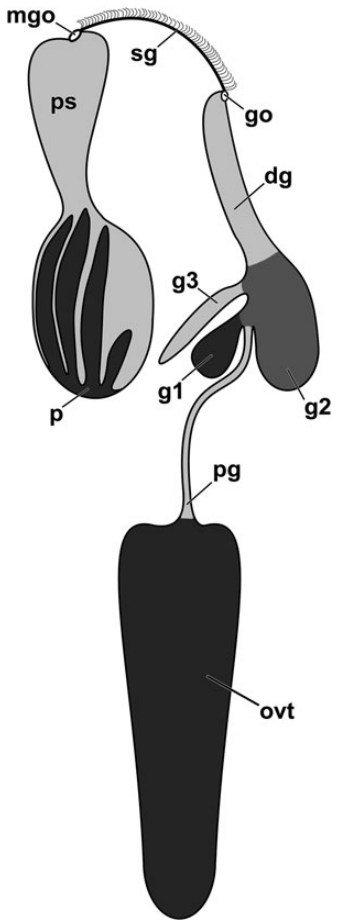


**Figure 10.** Schematic overview of genital system of *Creseis clava*. Abbreviations: dg, distal gonoduct; g1, genital accessory gland 1; g2, genital accessory gland 2; g3, genital accessory gland 3; go, genital opening; mgo, male genital opening; ovt, ovotestis; pg, proximal gonoduct; p, penis; ps, penial sheath; sg, sperm groove.

The foot of many euopisthobranchs carries lateral extensions (parapodia), which are sometimes used in swimming (Dayrat *et al*., 2001; Donovan Pennings & Carefoot, 2006), but it is still unclear if these are directly or completely homologous with the 'wings' of pelagic Pteropoda. Euthecosomes show two anterolaterally extending wings, which attach to the anterior part of the head, in close proximity to the mouth (Figs 2, 3B). These flat and extended wings constitute the primary locomotive organs, which characterize all euthecosomes (Lalli & Gilmer, 1989). They are also involved in the feeding process; euthecosomes feed by catching food with a spherical mucus web produced by the mantle gland; at intervals, this web is hauled in towards the mouth, using the ventral ciliated fields on the wings (Fig. 3B) (Lalli & Gilmer, 1989). According to Gilmer & Harbison (1968), some thecosomes, including *Creseis*, hang from this web upside-down, i.e. with the anatomically ventral side facing upwards. This coincides with the observation in the specimen examined here that the ciliated fields on the wings extend medioventrally along the surface of the wings, uniting directly under the mouth opening in an epidermal groove. This observation, however, differs from Meisenheimer's (1905) descriptions of the ciliated fields extending along the outer edge of the wings, without being associated with the mouth.

Meisenheimer (1905) described the foot of *Creseis* as clearly distinguishable from the wings; apparently this so-called 'foot' refers to the median footlobe mentioned herein. Judging from our material, the head of *Creseis* is not discernable as such, but appears completely fused with the foot, with unclear boundaries.

### *Mantle cavity*

The mantle cavity of *C. clava* is anatomically ventral, elongate and with an anterior opening. There is an anal opening and nephropore, but no gill or ciliary strips were detected. The walls of the mantle cavity possess two major glands, the mantle gland (or pallial gland) and anal gland. The former, located in the mantle roof (i.e. ventral) corresponds with the hypobranchial gland (e.g. van der Spoel, 1967) and exhibits some variation among thecosome species (Meisenheimer, 1905). The latter gland is small and located at the left anterior corner of the mantle cavity and is referred to as the 'anal gland' (e.g. Tesch, 1913) herein. van der Spoel (1967) noted its position distant from the anus and instead considered it homologous with the hypobranchial gland. The pigmented nature of the euthecosome anal gland indicates a potential homology with the pigmented mantle organ (see Dayrat & Tillier, 2002) of heterobranchs. In our material, this gland seems to be innervated by the thickest nerve of the left, larger ganglion of the visceral loop. The function of this organ is still unclear; based on its histology, Meisenheimer (1905) concluded that it most probably has either a glandular or a sensory function.

### *Digestive system*

Our 3D-model of *C. clava* visualizes and largely confirms the components of the digestive system that Meisenheimer (1905) found in Euthecosomata species. The digestive system of the Euthecosomata is generally subdivided into an anterior part located in the head cavity (consisting of the mouth opening, the pharynx, the radula, two salivary glands and the oesophagus) and a posterior part extending through the entire visceral sac, which is comprised of the gizzard with gizzard plates, the digestive gland, a caecum and the intestine (Meisenheimer, 1905). Among the Euthecosomata the radula usually shows *c.*10 rows, each carrying two thin hook-shaped lateral teeth and a pointed, serrated and triangular middle tooth (van der Spoel, 1967). The radula formula was detectable even in our 3D-reconstructed specimen, which, however, shows only three rows of radula teeth (Fig. 5A).

The very small and short salivary glands found here in *C. clava* are attached laterally to the pharynx; salivary ducts could not be discerned. This coincides with Meisenheimer's (1905) descriptions of *Creseis* and *Hyalocylis*, in which he identified two very small glands comprised of only 2–3 cells that connect laterally to the buccal apparatus; in contrast, other Euthecosomata, such as *Cuvierina* species, feature large and extensive salivary glands (Meisenheimer, 1905).

The oesophagus of *Creseis* is longer than that of other euthecosomes (Meisenheimer, 1905; this study). The epithelium of the oesophagus is characterized by ciliated cells along most of its length and features multiple longitudinal folds (Fig. 5B). This distinctive arrangement was also observed in *C. clava* and all Euthecosomata by Meisenheimer (1905), who also stated that the epithelium is more convoluted towards the end of the oesophagus; in our material, it is the other way around.

*Creseis* and other thecosomes have a gizzard, a character that was considered a synapomorphy of Euopisthobranchia by Jörger *et al*. (2010). In *C. clava*, the gizzard contains four large and one small gizzard plate, the smaller plate being situated ventrally and slightly shifted to the posterior end of the other plates. Meisenheimer (1905) observed the same arrangement of the plates in most euthecosome species except for *Limacina*, where the single plate is situated dorsally. This finding may be explained by the concept of de-coiling introduced by Boas (1886), hypothesizing that straight-shelled Euthecosomata (such as *Creseis*) feature a visceral sac inverted relatively to the head, in

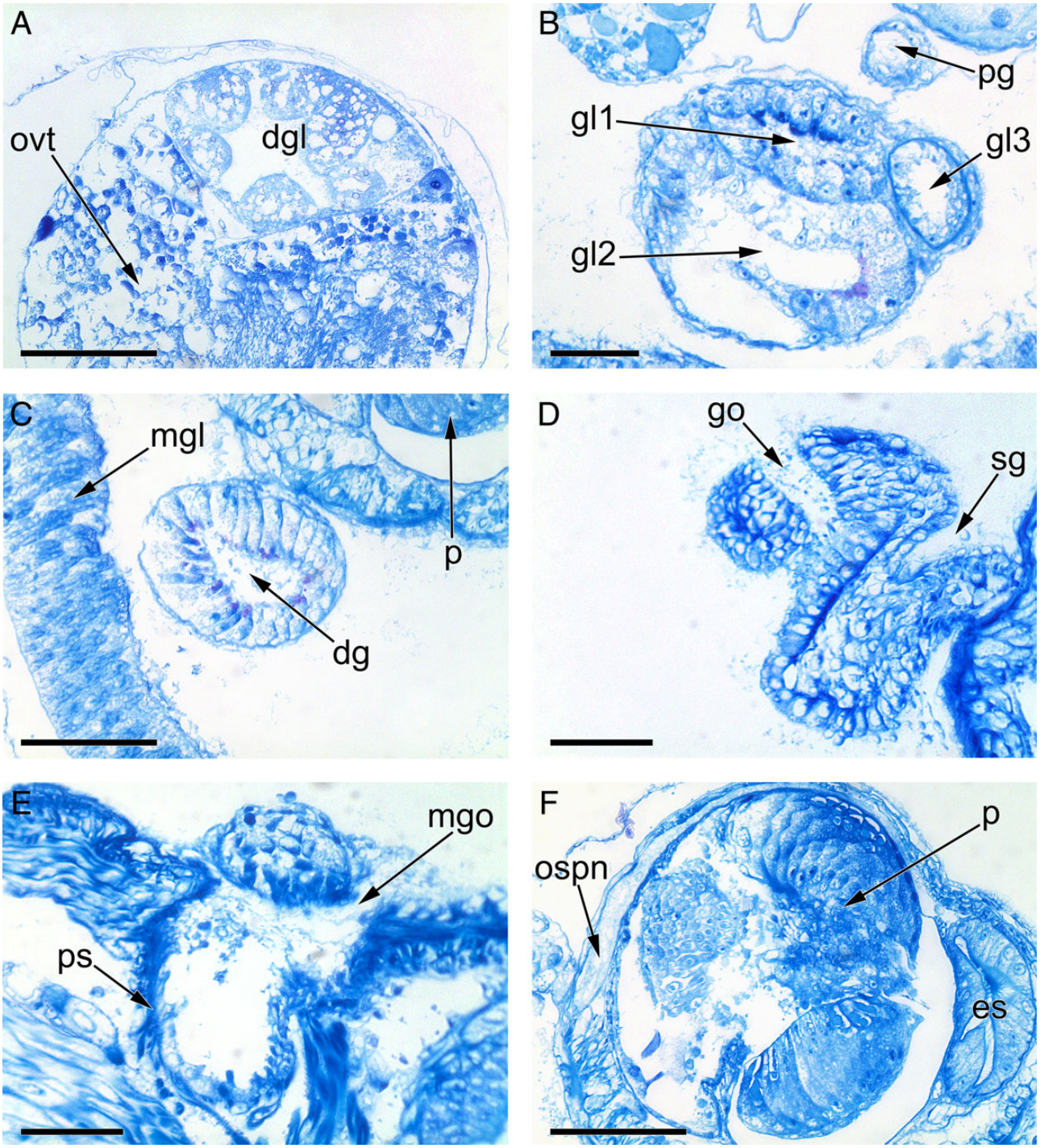


**Figure 11.** Semithin cross sections of the genital system of *Creseis clava*. **A.** Posterior visceral sac filled in large part by ovotestis. **B.** Cross section of the genital accessory glands. **C.** Distal gonoduct. **D.** Genital opening and adjacent epidermal sperm groove. **E.** Penial sheath connected to male genital opening. **F.** Male copulatory organ. Abbreviations: dg, distal gonoduct; dgl, digestive gland; es, oesophagus; go, genital opening; gl1, genital accessory gland 1; gl2, genital accessory gland 2; gl3, genital accessory gland 3; mgl, mantle gland; mgo, male genital opening; ospn, osphradial nerve; ovt, ovotestis; p, penis; pg, proximal gonoduct; ps, penial sheath; sg, sperm groove. Scale bars: **A, C, F** = 50 μm; **B, D, E** = 25 μm.

contrast to coiled-shelled Euthecosomata such as *Limacina*. This was explained by a rotation of the visceral sac by 180° along its longitudinal axis, thereby relocating the mantle cavity to the ventral side and rotating some, but not all, internal organs. For example, as can be seen from the 3-D model, the digestive gland of *C. clava* is situated on the right side of the body (as in all straight-shelled euthecosomes), whereas in coiled-shelled species (such as in *Limacina*) it is situated on the left side (Meisenheimer, 1905).

The digestive gland of *C. clava* extends into the tip of the strongly elongated visceral sac. Meisenheimer (1905) observed that the gland features almost no (internal) lobes in *C. clava* (in contrast to other related species) and assumed that this was due to its strongly elongated body and digestive gland. Our results

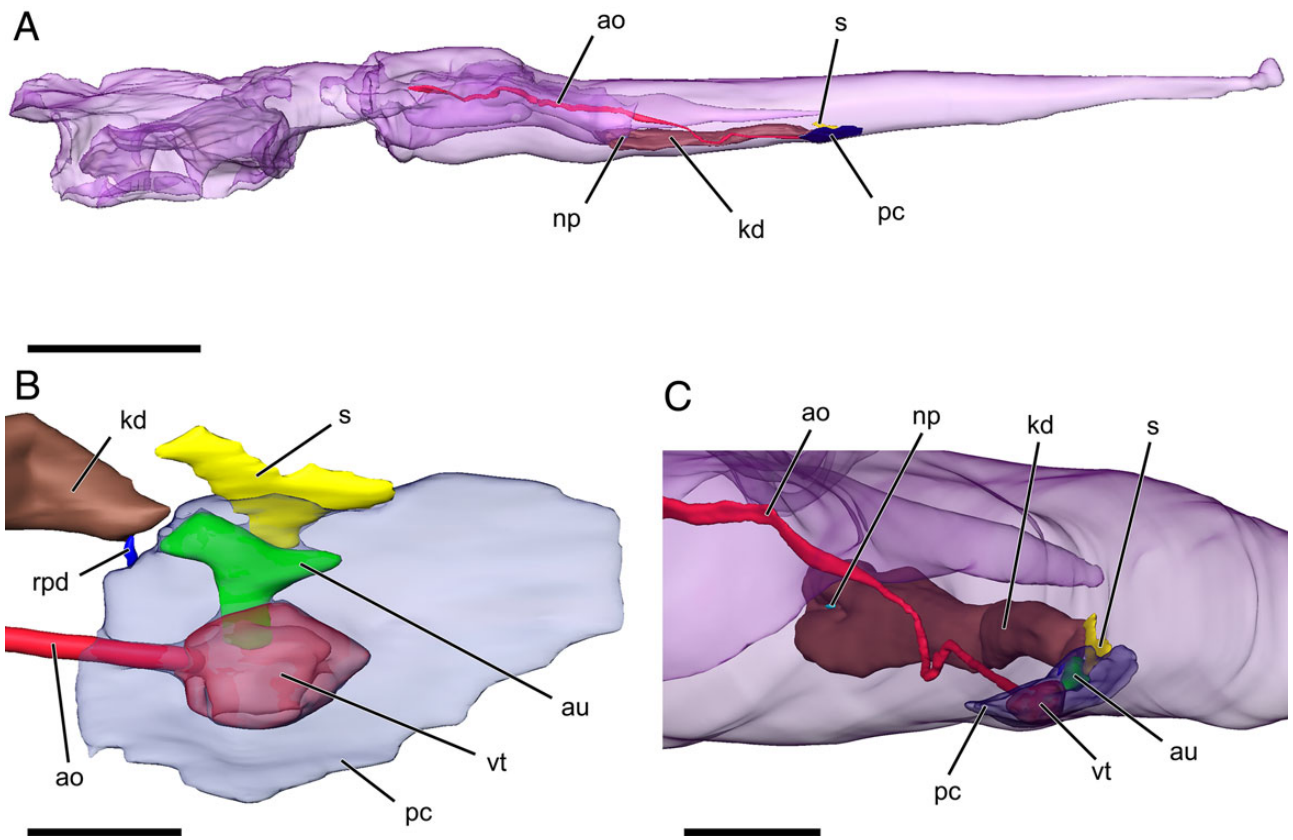


**Figure 12.** 3D-reconstruction of circulatory and excretory systems of *Creseis clava*. **A.** Localization of circulatory and excretory system within the specimen, left lateral view. **B.** Heart and renopericardial system, dorsal view. **C.** Heart and renopericardial complex, left posterolateral view. Abbreviations: ao, aorta; au, auricle; kd, kidney; np, nephroporus; pc, pericard; rpd, renopericardioduct; s, haemolymph sinus; vt, ventricle. Scale bars: **A** = 500 μm; **B** = 50 μm; **C** = 100 μm.

contradict previous data in that the reconstructed specimen possesses a large quantity of digestive lobes, densely packed around the gland's central lumen; most cells have a granular cytoplasm in accordance to their secretional and resorptive function in digestion (Meisenheimer, 1905).

*Creseis clava* possesses a tubular, highly ciliated caecum-like structure, which is closely attached to the digestive gland (Meisenheimer, 1905). This caecum is situated on the left side of the digestive gland in coiled-shelled Euthecosomata and on the right side in straight-shelled Euthecosomata, as in *C. clava* (Meisenheimer, 1905; this study). The function or homology of thecosome caeca is still unclear. Whether or not this caecum is the remainder of a style sac as in some caenogastropods (e.g. Fretter & Graham, 1962), or a reduced and specialized right branch of a paired digestive gland, as hypothesized for nudibranchs by Schmekel & Portmann (1982), remains to be studied.

The intestine, which branches from the stomach, features a loop in close proximity to the digestive gland and opens through the anus into the mantle cavity (Fig. 3D). In coiled-shelled species such as *Limacina*, this loop turns slightly towards the right side of the body, whereas in uncoiled orthoconchs it loops towards the left side (Meisenheimer, 1905; this study, Fig. 3D). The histology of the intestine found in our material coincides in large parts with Meisenheimer's descriptions. In all Euthecosomata the intestine has a longitudinal internal fold (Fig. 5F), differing in size depending on the species (Meisenheimer, 1905). Specifically in *C. clava*, Meisenheimer (1905) also identified a similar, unilateral ridge of the intestine's epithelium. He assumed that this cell enlargement increases the resorptive ability of the intestine by enlarging the epithelial surface, in analogous fashion to a typhlosole in other invertebrates; however, we assume that it is rather related to effective transport of faeces, because the intestine does not possess a particular resorptive function in molluscs.

### *Nervous system*

The 3D-reconstruction of the CNS of *C. clava* demonstrates its highly concentrated nature, comprising an anterior nerve ring and a short visceral loop, with all ganglia closely attached to each other. This configuration corresponds in most respects to the CNS of other Euthecosomata species described by Meisenheimer (1905) and as shown by Franc (1968: fig. 398c). The presence of two separate, putative cerebropedal and pleuropedal connectives confirms the fused nature of the paired, anterodorsal cerebropleural ganglia in *Creseis*; there is not a merely superficial separation between the cerebral and the pleural ganglia, as in *Cuvierina* (Meisenheimer, 1905; this study). Furthermore, the buccal ganglia are fused as are those of the visceral loop; only the pedal ganglia appear not to be fused in any way.

### *Nerve ring*

In the elongate cerebropleural ganglia, we were able to detect a single, anterior pair of cerebral nerves, dividing into two branches and innervating areas of the pharynx, with a branch that is tentatively interpreted as the oral (labial) nerve. The other branch leads anteriorly, apparently also innervating the anterior part of the penis. Meisenheimer (1905) roughly described these nerves in *Creseis*, but as innervating exclusively the pharynx and areas around the mouth opening, without

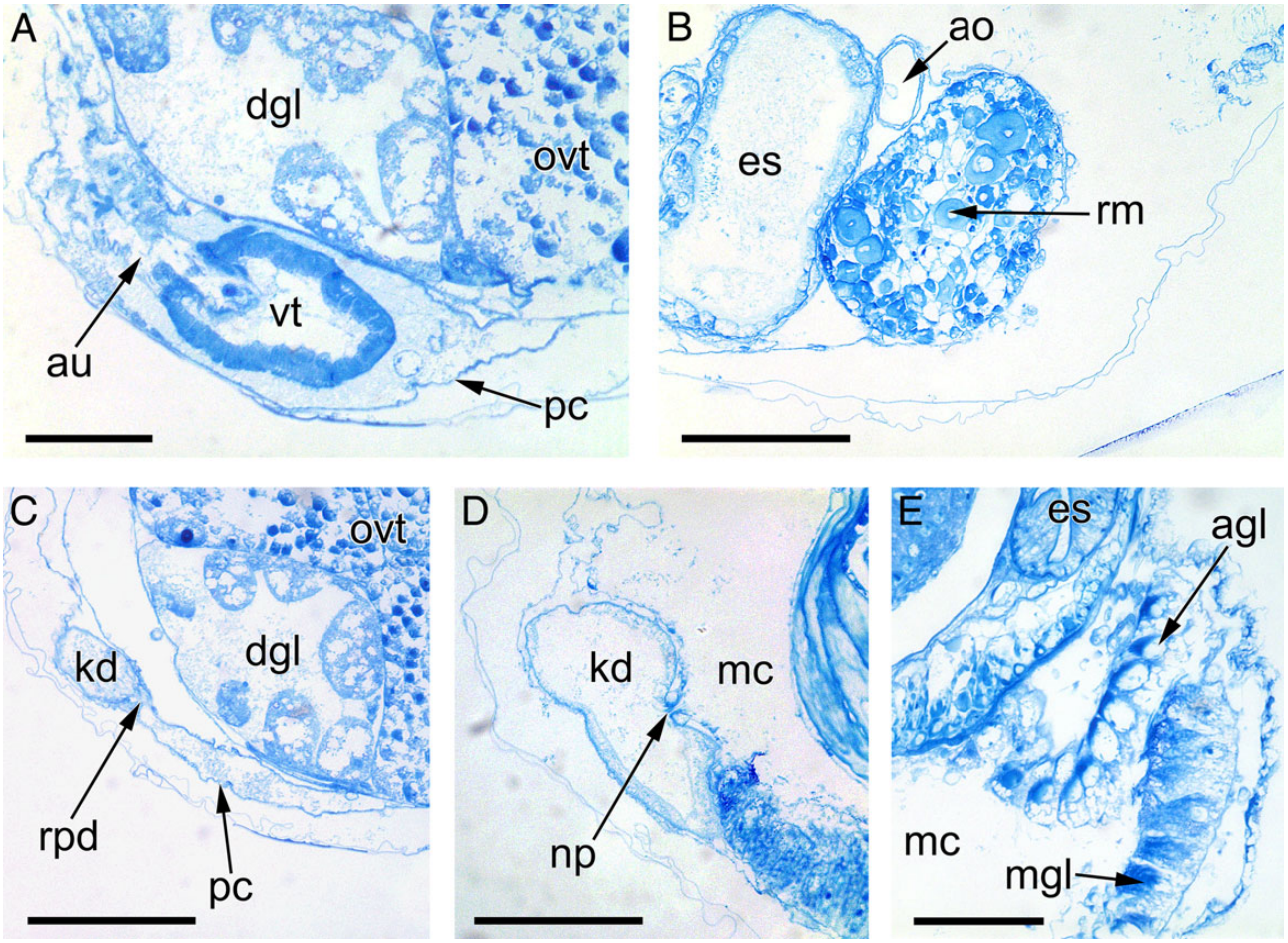


**Figure 13.** Semithin cross sections showing aspects of circulatory and excretory systems and mantle cavity gland of *Creseis clava*. **A.** Cross section of the heart at junction of auricle and ventricle. **B.** Aorta in anterior part of visceral sac. **C.** Connection of pericardium and kidney (renopericardial duct). **D.** Nephropore. **E.** Cross section of anal gland. Abbreviations: agl, anal gland; au, auricle; ao, aorta; dgl, digestive gland; es, oesophagus; kd, kidney; mc, mantle cavity; mgl, mantle gland; np, nephropore; ovt, ovotestis; pc, pericardium; rm, retractor muscle; rpd, renopericardioduct; vt, ventricle. Scale bars: **A** = 25 μm; **B–D** = 50 μm; **E** = 40 μm.

mentioning innervation of the penis. In *Clio pyramidata*, cerebral nerves apparently do not innervate the penis; instead they lead only into parts of the exterior head region and into the wing protrusions (Meisenheimer, 1905). Static or optic nerves were not detected in our material, but are usually very thin and difficult to discern. In general, euthecosomes have been reported to possess three pairs of cerebral nerves, namely the static nerves, labial nerves and tentacular nerves (Huber, 1993).

Huber (1993) stated that the tentacles of caenogastropods, 'archaeopulmonates' and, among others, thecosomes are innervated by the nervus tentacularis, which he homologized with the nervus clypeus capitis of the Cephalaspidea. In contrast, Staubach (2008) showed the nervus tentacularis of the caenogastropod *Littorina* to be composed of the labiotentacular and rhinophoral nerves; the nervus clypei capitis does not innervate any tentacles in the studied opisthobranchs and (pan)pulmonates (Klussmann-Kolb, Croll & Staubach 2013; Koller, Brenzinger & Schrödl, 2014). Meisenheimer (1905) reported that the tentacular nerve innervates the (posterior) 'tentacles' of thecosomes, but did not give details about the innervation of the 'wing protrusions' (anterior tentacles). We tentatively interpret the cerebral nerves in thecosomes to be combined rhinophoral and labiotentacular nerves innervating the rhinophores and, potentially, the anterior tentacles; the latter we regard as homologues with the labial (or oral) tentacles present in gymnosomes, anaspideans and some other euopisthobranchs, as well as in nudipleurans and many panpulmonates. More detailed studies are needed to confirm the exact innervation of the putative labial tentacles of thecosomes by a branch of the tentacular nerve. The 'labial' nerve of thecosomes may be homologous with the oral nerve ('N1'; e.g. Staubach *et al.*, 2008; Klussmann-Kolb *et al.*, 2013), but its target area needs to be investigated. Interestingly, Huber (1993) considered that the presence of a tentacular nerve in adult Thecosomata reflects a retained larval condition, i.e. an apomorphic paedomorphosis, rather than a plesiomorphic feature in common with caenogastropods. Recent hypotheses on heterobranch phylogeny recover Thecosomata as a derived euopisthobranch clade (Klussmann-Kolb & Dinapoli, 2006; Jörger *et al.*, 2010; Wägele *et al.*, 2014) and thus support this view.

The pedal ganglia are interconnected in the reconstructed specimen by only one short and thick pedal commissure; we could not discern an additional, much narrower parapedal commissure as reported in *Creseis* and other euthecosomes by Meisenheimer (1905) and Tesch (1913). *Creseis clava* studied herein shows that each pedal ganglion gives rise to three large nerves. The thickest of these nerves runs to the base of the wings and innervates them through all of their length; the two smaller nerves could not be followed in our specimen. Meisenheimer (1905), in *C. pyramidata*, ascribed four nerves to each pedal ganglion; Franc (1968) counted up to five pairs. The thickest of

**Table 1.** Comparison of the positions of particular organs in *Creseis* and *Limacina*.

| 3D-model *Creseis clava* | *Creseis* | *Limacina* |
|---|---|---|
| Mantle cavity → ventral | Ventral | Dorsal |
| 5th gizzard plate → ventral | Ventral | Dorsal |
| Digestive gland → right | Right | Left |
| Caecum → right | Right | Left |
| Intestine loop → left | Left | Right |
| Anus → medial | Left | Right |
| Osphradium → right | Right | Left |
| Visceral ganglion → left | Left | Right |
| Genital opening → right | Right | Right |
| Heart → medial | Right | Left |
| Kidney → right | Right | Left |
| Mantle gland → ventral | Ventral | Dorsal |
| Mantle cavity gland → left | Left | Right |

Left column: traits identified in 3D-reconstruction of *C. clava*.
Middle column: traits observed by Meisenheimer (1905) in *Creseis*.
Right column: traits observed by Meisenheimer (1905) in *Limacina*.

these nerves was reported to run into the wings, almost to their anterior edge (Meisenheimer, 1905); this corresponds to our observations in *C. clava*. In *Clio*, the remaining three pedal nerves run into different target areas, such as the base of the wings and the epidermal groove around the mouth opening. The lobes surrounding this structure were therefore defined as foot-lobes by Meisenheimer (1905). The three smaller pedal nerves described by Meisenheimer could not be correlated individually with the two smaller pedal nerves found in this study.

In *C. clava*, we found the buccal ganglia to be connected with both cerebropleural ganglia via short connectives; no visible separation of the cortices of the (ancestrally paired) buccal ganglia could be recognized. This observation coincides in large part with Meisenheimer's (1905) findings. Only in *H. striata* did he recognize a rudimentary inner separation of the buccal ganglia through a visible division of the perikarya. Most species of Euthecosomata have completely fused buccal ganglia, which is a potential apomorphy for the Euthecosomata.

Of the three nerves that emerge anteriorly from the buccal ganglia according to Meisenheimer (1905) and Franc (1968), only two could be found in the reconstructed specimen. These two nerves run exactly as described for the three nerves Meisenheimer identified, i.e. anteriorly towards the mouth region, clearly innervating the pharynx from both sides.

### *Visceral loop*

The highly concentrated and obviously fused composition of the ganglia situated on the visceral loop in *C. clava* coincides with the condition reported in other species of Euthecosomata (Meisenheimer, 1905). According to hypotheses on the development of the CNS of Heterobranchia (Haszprunar, 1985), the visceral loop can be assumed to originate from either three or five separate anlagen during ontogeny. In adult euthecosomes, only two ganglia can be distinguished throughout all species, one on the right side of the visceral loop and one on its left side (Meisenheimer, 1905; Franc, 1968). In *Creseis*, the right ganglion is smaller than the left, whereas in the helicoid *Limacina*, it is the other way round (Meisenheimer, 1905). This may imply opposing patterns of fusion in these two taxa, as reported by Franc (1968). Tesch (1913) identified the right ganglion as the supraoesophageal ganglion, and the left one as the product of fusion of the abdominal (= visceral) and suboesophageal ganglia. This interpretation is supported by our observation of a rudimentary yet discernible internal separation of the left ganglion through the arrangement of the perikarya. Meisenheimer (1905) observed the same intrusion of the cortical perikarya into the inner medulla in *Diacria*; in *Clio* and *Cavolinia* this internal separation was less distinctive. This similarity may indicate that the latter two genera are more closely related to each other than to *Diacria* and *Creseis*, which show a presumably ancestral (i.e. less fused) pattern. Once the polarity of characters has been clarified among thecosomes and related euopisthobranchs, such morphological information could, in addition to genetic analyses, be useful to investigate ambiguous phylogenetic relationships (see Corse *et al.*, 2013), specifically between *Diacria*, *Cavolinia* and *Clio*.

In the reconstructed specimen the right visceral loop ganglion dispatches one nerve towards the right side of the mantle, connecting to the elongated osphradial ganglion, which is situated directly below the osphradium (Figs 6B, 7, 8F). Therefore, the right visceral loop ganglion corresponds to, or at least contains parts of, the supraoesophageal ganglion (see Brenzinger *et al.*, 2013b for discussion of euthyneuran nervous systems). The double innervation of the osphradium and right mantle side by this right ganglion is in agreement with Tesch's (1913) observation on *Creseis* (see also Franc, 1968: fig. 398) and coincides in most respects with Meisenheimer's (1905) descriptions. However, the latter author did not mention any looping osphradial nerve in any of the euthecosome species investigated, which could be due to the fact that eversion of the penis and penial sheath could change the conformation at least of the loop of the osphradial nerve.

The osphradium is an unpaired chemosensory organ typically situated on the inner wall of the apogastropod mantle cavity in the anterior part of the visceral sac (e.g. Haszprunar, 1985, 1988). In all coiled euthecosomes, it is located on the left side of the body, whereas in straight-shelled species it is on its right side (Meisenheimer, 1905) (Figs 6A, 7). This was confirmed by the 3D-model of *C. clava*. In all Euthecosomata the osphradium is characterized by an elongated, flat and ciliated stretch of epithelium, under which an osphradial ganglion of equal dimensions is located (Meisenheimer, 1905).

Two nerves emerge from the left, larger visceral loop ganglion of *Creseis*. As reported for *C. pyramidata* (Meisenheimer, 1905), one of the two nerves is rather narrow and proceeds towards the visceral sac, running along the digestive tract towards the posterior part of the visceral sac, where the genital organs are situated, while presumably innervating both organ systems. This is largely in agreement with Tesch's (1913) observation that there are two nerves emerging from the inner part of the visceral loop (a visceral and a genital nerve); these separate nerves may be the same as the aforementioned single nerve found in our material. The second, thicker nerve runs laterally along the left side of the mantle towards the anterior part of the visceral sac (Meisenheimer, 1905; Tesch, 1913). In contrast to the observation of Meisenheimer, who stated without any further explanation that the thick nerve's target organ is the right side of the mantle, we identified the mantle cavity gland as its target organ.

The left, putatively fused visceral loop ganglion is larger than the right ganglion, and it gives rise to two nerves. Innervating visceral organs, the euthyneuran visceral ganglion may contribute to this fused ganglion; its other portion is tentatively referred to as the suboesophageal ganglion, pointing to an at least triganglionate condition. There is not yet any indication of a pentaganglionate condition (with additional, separate or fused parietal ganglia) (see Haszprunar, 1985) in thecosomes.

Concluding, the CNS of *Creseis* is characterized by strong condensation and various assumed fusions among ganglia, such as between the cerebral and the pleural ganglia, the two buccal

ganglia and between those of the visceral loop (Meisenheimer, 1905). Further examination of nervous systems of pteropods and related euopisthobranchs is needed to infer their homologies, functions and evolution, e.g. with relation to the reduction of the head and tentacles and their potential integration into predominately pedally innervated wings. The wings thus appear to be specialized parts of the foot transformed to function in swimming.

### *Reproductive system*

*Creseis clava* possesses a monaulic genital system and is a protandric hermaphrodite, as was shown by the presence of male sexual organs in early stages of life and both male and female sexual organs in older individuals (Meisenheimer, 1905); the male gonad portion is in large part replaced by the female one. The reconstructed specimen of *C. clava* was fixed in a hermaphroditic stage, possessing both female genital glands and a penis. We could distinguish only a few eggs or egg-like cells with a yolky cytoplasm, situated mostly in the periphery of the ovotestis. Meisenheimer depicted the sperm-producing tissue in one of his sketches, as a tissue constituted of closely packed dark dots. A similar observation was made in the reconstructed specimen, identifying in the centre of the ovotestis very small areas of dark blue stained dots (Fig. 11A); these are, however, not unequivocally spermatozoa.

The gonoduct is a long, narrow, tubular structure that transports the gametes to the complex of genital glands. The gonoduct features a ciliated epithelium (Meisenheimer, 1905), which, however, could not be clearly identified as such in our specimen. Meisenheimer observed throughout all the Euthecosomata that the proximal gonoduct is differentiated from the rest as an ampulla that stores mature autosperm until copulation. Specifically in *Creseis*, Meisenheimer (1905) described it as a caecum-like evagination of the gonoduct, located immediately next to the connection of the latter to the ovotestis. No such structure could be recognized in our specimen.

The complex of genital glands, through which the more distal gonoduct leads dorsally, consists of three glandular, epithelial structures (here called glands 1–3). The complex of genital glands is found in all Euthecosomata on the right side in the anterior part of the visceral sac (Meisenheimer, 1905). This position was also confirmed in the 3D-model of *C. clava*. The interconnections of the single genital glands and the gonoduct differ among species of the Euthecosomata (Meisenheimer, 1905). Meisenheimer described these interconnections thoroughly for *C. clava*; his observations coincide in most but not all respects with our own. Meisenheimer attributed to glands 1 and 2 a function in the preparation and coating of fertilized eggs, directly after copulation. Gland 1 thus could be homologous with the capsule gland identified by Klussmann-Kolb (2001) in nudibranchs. Gland 2 has a ciliated epithelium according to Meisenheimer (1905), which could not be seen in the reconstructed specimen, and could be a mucus gland. As shown in the 3D-model, gland 2 is long and tubular, proceeding into a narrower duct-like structure, which represents the distal gonoduct (Meisenheimer, 1905). This transports the gametes to the genital opening, which is located on the right side of the mantle cavity floor. The bag-like gland 3 was characterized by a slight muscular layer and a ciliated epithelium, and was identified as a receptaculum seminis (Meisenheimer, 1905) or vesicula seminalis (Tesch, 1913) by earlier workers. While these histological observations were confirmed in our specimen, we do not agree with previous interpretations: gland 3 does not contain any sperm and does not resemble a typical receptaculum or bursa as described by Wägele & Willan (2000). Its identity and function as a sperm-receiving receptacle needs further investigation.

Herein we confirm the presence of a seminal groove in *C. clava*. A monaulic genital system with open sperm groove is typical for euopisthobranchs and was long regarded as plesiomorphic for opisthobranchs in general (but see Schrödl *et al.*, 2011; Brenzinger *et al.*, 2013a). Monauly is clearly plesiomorphic for pteropods and thecosomes, but the androdiaulic condition has evolved at least once. *Cavolinia* is the only genus among the Euthecosomata that does not feature an open seminal groove, but instead a closed vas deferens, as described by Meisenheimer (1905). The closed vas deferens is an apomorphy for *Cavolinia*, which forms the most derived clade within Orthoconcha together with *Diacria* and *Clio* (Corse *et al.*, 2013). The arrangement of the vas deferens in *Cavolinia* is similar to the 'special androdiaulic' condition in panpulmonate acochlidian hedylopsaceans (Schrödl *et al.*, 2011) and obviously evolved convergently.

In *Creseis*, the penis is a complex infolded organ, enveloped by a sheath that connects to the seminal groove apically. The entire copulatory organ fills a considerable part of the head cavity in all euthecosome species except for *Cavolinia* (Meisenheimer, 1905). As described by Meisenheimer for *C. clava*, the penis sheath is attached to the long retractor muscle at its posterior end; this muscle extends to the most posterior end of the visceral sac (Fig. 9A). In both Meisenheimer's (1905) study of *C. clava* and our own, a long, narrow, putatively muscular structure was found which could not be allocated to any other organ systems. We suspect this is a homologue of the columellar muscle retracting the headfoot and buccal mass, but connections could not be seen as a result of local damage of tissues.

As described by Meisenheimer (1905), all Thecosomata except for the genus *Cavolinia* possess complex copulatory organs with stylets. The penis of *C. clava* features several side branches (caeca) that are filled with extensive glandular organs. We did not find stylets in the single specimen investigated, and the number of caeca and their ramifications could not be definitely determined. The functions of these structures (caeca, stylets and side branch) remain unclear. *Creseis* was reported to copulate reciprocally, with wings of partner intertwined and their penises connecting externally (Lalli & Gilmer, 1989: p. 109), which is similar to the condition in terrestrial stylommatophoran slugs such as *Limax*, although here the 'penises' are in fact composed of male and female gonoducts. In *Creseis* and other euthecosomes, the male copulatory organ stands alone and usually in a frontal position; this implies that there is no contact with the more posterior 'female' genital opening during copulation, so we suggest that the lateral caeca of the penis could act as temporary allosperm-receiving structures. Copulatory organs, however, show some structural variation among euthecosomes, which could be of taxonomic relevance; for example, the copulatory organ of *Diacria* species has been reported to be very large compared with the animal itself (Lalli & Gilmer, 1989). Similar copulatory organ systems that are particularly large, complex and bear stylets and accessory glands, are known from several euthyneuran groups (Sanders-Esser, 1984; Kohnert *et al.*, 2010; Brenzinger *et al.*, 2011a) and could indicate traumatic mating and sexual conflict (e.g. Lange, Werminghausen & Anthes, 2013), or possibly divergence within widespread pelagic populations as a result of sexual selection (Churchill *et al.*, 2013).

### *Circulatory and excretory systems*

Meisenheimer's (1905) findings regarding the renopericardial complex in Euthecosomata were reexamined and in large part confirmed in *C. virgula* by Fahrner & Haszprunar (2000). The main components of the circulatory system are the aorta and a monotocardian heart, consisting of a ventricle and a single auricle. The heart is enveloped by a thin-walled pericardium, which is connected to the kidney via a renopericardioduct. As the 3D-reconstruction indicates (Fig. 12B, C) the heart of *C. clava* is

situated medioventrally halfway through the visceral sac, although described as situated on the right side by Franc (1968), which may indicate some artificial twisting of retracted specimens. This is also suggested by the fact that in our 3D-model the ventricle and auricle are arranged side by side, with the ventricle on the left (agreeing with Fahrner & Haszprunar, 2000), while described as antero-posterior (longitudinal) by Meisenheimer (1905). Only in the case of *Cuvierina* and *Hyalocylis* did Meisenheimer describe a transverse arrangement of the ventricle and the auricle.

As shown for *Creseis* by previous authors, the main components of the excretory system are the auricle wall (where the actual ultrafiltration into the pericardium takes place) and the kidney (where processing of the primary urine occurs) and the renopericardial duct features a ciliated epithelium (Meisenheimer, 1905; Fahrner & Haszprunar, 2000). This general arrangement was confirmed here for *C. clava*.

### *Taxonomic remarks*

We identified our specimen as *C. acicula* which, according to Gasca & Janssen (2014), is a junior synonym of *C. clava*, because of its distinctive elongate shell. *Creseis virgula*, in contrast, was reported to possess a stouter, curved shell. Using the barcoding region of the COI gene as a sequence marker, Gasca & Janssen (2014) supported the specific distinction of elongate *vs* stout shell morphs. However, their *C. acicula* is paraphyletic with regard to *C. clava* in the COI tree (Gasca & Janssen, 2014) and there appears to be geographical structure. In particular, basal *C. acicula* lineages are Indo-Pacific, while the remaining clade combines specimens of *C. clava* and *C. acicula*, all from the Caribbean. We believe that considerable variation exists in *Creseis* shell shapes, and potentially also in soft-part characters, as indicated herein, so that further analyses of intraspecific *vs* interspecific variation is required. We also doubt that single pteropod species occur across oceans and hydrogeographic boundaries (Uribe *et al*., 2013). Recent molecular studies have revealed complexes of cryptic species within traditionally shell-based thecosome taxa (Hunt *et al*., 2010; Birky, 2013; Maas, Blanco-Bercial & Lawson, 2013). Higher species diversity than expected from traditional taxonomy, and more limited ranges than predicted from high dispersion ability, have been discovered in other pelagic sea slugs also (Churchill *et al*., 2014). Externally cryptic species of the nudibranch *Glaucus marginatus* complex show distinctly different reproductive organs, with a bursa developed or not, and sexual selection was hypothesized to drive speciation within wide-ranging pelagic sea slugs (Churchill *et al*., 2013). Recent results emphasize a high level of cryptic species with narrower than expected ecological and distributional ranges in other holoplanktonic groups also, such as calanoid copepods (Cornils & Held, 2014). An integrative and global approach, as performed by Jörger *et al*. (2012) for the acochlidian sea slug genus *Pontohedyle*, could be useful to resolve species limits within *Creseis*.

### *Orthoconchy via detorsion?*

In general, helicoid thecosomes have a dorsal mantle cavity (Meisenheimer, 1905). In contrast, *Creseis* and other straight-shelled thecosomes (Orthoconcha) have a ventral mantle cavity, opening ventrally to the mouth. This condition implies a rotation of the visceral sac relative to the (reduced and transformed) headfoot by 180° along the longitudinal body axis. A comparison of other organ systems (Table 1) is consistent with this assumption. Where present in euopisthobranch gastropods, the mantle cavity is dorsal; a rotation of 180° to the ventral side, as envisioned by Boas (1886), would thus be a synapomorphy of orthoconch thecosomes. Relative rotation can be explained by secondary detorsion of the mantle and viscera, or by more or less impeded torsion. The latter appears likely according to descriptions of some ontogenetic stages of *Creseis* by Gegenbaur (1855), in which no major torsion or detorsion events were indicated. Boas (1886) also assumed that orthoconchs are decoiled. However, the apparently uncoiled nature of *Creseis* larvae (Gegenbaur, 1855) implies that a rather symmetrical, uncoiled body is present throughout orthoconch ontogeny. The lack of evident torsion and coiling in orthoconchs may be considered paedomorphic, produced by abbreviated or skipped developmental processes (which are active in coiled limacinids) and a derived condition, because limacinid shells appear earlier in the fossil record than straight shells (Corse *et al*., 2013). The relocation of the mucus-web forming mantle gland below the foot and mouth possibly provides a more efficient way of mucus-web feeding, or facilitates faster jettisoning of the web during escape from predators.

## CONCLUSION

This is an initial study of thecosome microanatomy, providing data from *Creseis clava* for future comparisons with other pteropods and euthyneurans. In most respects, our results confirmed Meisenheimer's (1905) descriptions. In addition, our approach allowed for discovery of several additional details, such as those of central nervous structures, gizzard and genital organs. We also provide some first opinions on homologies of thecosome organs, in particular of cerebral nerves and tentacles, in the light of modern structural and phylogenetic hypotheses. However, our observations and assumptions will need confirmation and supplementation through study of additional and better fixed specimens, ideally of different ontogenetic stages.

We have used our data for comparison of *Creseis* (as a supposedly basal member of Orthoconcha) with other straight-shelled euthecosomes and with limacinids such as *Limacina* having helicoid shells. Both straight shells and unusually rotated posterior organs intuitively suggest that these special features of Orthoconcha are apomorphic relative to supposedly plesiomorphic *Limacina*-like thecosomes (Corse *et al*., 2013) and are functionally and/or evolutionarily related. This remains to be confirmed in the light of reliable hypotheses of thecosome phylogeny.

We hypothesize that the symmetrical, uncoiled and untorted body of larval to adult *Creseis* is produced by skipping the developmental processes of torsion and coiling, and are therefore paedomorphic features. In addition, previous authors have proposed the retention of a bifurcate tentacular nerve (Huber, 1993) and of a permanent, continuously growing functional larval shell (Haszprunar, 1985) as paedomorphic features of thecosomes. We may add to this list an incomplete differentiation and separation of the head (with more or less reduced or transformed tentacles including parts of the cerebral larval velum) and foot, allowing for transformation of the combined headfoot into the charismatic thecosome wings. Confirming and supplementing old ontogenetic descriptions of thecosomes, gymnosomes and related outgroups will be necessary for assessing heterochronic processes that have driven thecosome evolution.

## ACKNOWLEDGEMENTS

Alexander Fahrner (Landsberg) and the staff of the Hydra Institute are thanked for their assistance in collecting specimens in Elba. Many thanks go to Eva Lodde-Bensch (ZSM), who embedded and serially sectioned the specimen. Amira licenses and hardware were provided by the GeoBioCenter LMU and via DFG SCHR667/9 and 13. The organizers of the World Congress of Malacology 2013 and of the opisthobranch symposium are warmly thanked.

## REFERENCES


BEDNARŠEK, N., FEELY, R.A., REUM, J.C., PETERSON, B., MENKEL, J., ALIN, S.R. & HALES, B. 2014. *Limacina helicina* shell dissolution as an indicator of declining habitat suitability owing to ocean acidification in the California Current Ecosystem. *Proceedings of the Royal Society*, **281**. doi: 10.1098/rspb.2014.0123.

BIRKY, C.W., Jr. 2013. Species detection and identification in sexual organisms using population genetic theory and DNA sequences. *PLoS ONE*, **8**: e52544.

BOAS, J.E.V. 1886. Spolia Atlantica. bidrag til pteropodernes, morfologi og systematik samt til kundskaben om deres geografiske udbredelse. *Kongelige Danske Videnskabernes Selskabs Skrifter, Naturvidenskabelig og Mathematisk Afdeling*, **6**: 1–231.

BRENZINGER, B., HASZPRUNAR, G. & SCHRÖDL, M. 2013b. At the limits of a successful body plan—3D microanatomy, histology and evolution of *Helminthope* (Mollusca: Heterobranchia: Rhodopemorpha), the most worm-like gastropod. *Frontiers in Zoology*, **10**: 37.

BRENZINGER, B., NEUSSER, T.P., JÖRGER, K.M. & SCHRÖDL, M. 2011a. Integrating 3D-microanatomy and molecules: natural history of the Pacific freshwater slug *Strubellia* Odhner, 1937 (Heterobranchia: Acochlidia), with description of a new species. *Journal of Molluscan Studies*, **77**: 351–374.

BRENZINGER, B., PADULA, V. & SCHRÖDL, M. 2013a. Insemination by a kiss? Interactive 3D-microanatomy, biology and systematics of the mesopsammic cephalaspidean sea slug *Pluscula cuica* Marcus, 1953 from Brazil (Euopisthobranchia: Cephalaspidea: Philinoglossidae). *Organisms, Diversity and Evolution*, **13**: 33–54.

BRENZINGER, B., WILSON, N.G. & SCHRÖDL, M. 2011b. 3D microanatomy of a gastropod 'worm', *Rhodope rousei* n. sp. (Heterobranchia) from Southern Australia. *Journal of Molluscan Studies*, **77**: 375–387.

CHURCHILL, C.K.C., ALEJANDRINO, A., VALDÉS, Á. & Ó FOIGHIL, D. 2013. Parallel changes in genital morphology delineate cryptic diversification of planktonic nudibranchs. *Proceedings of the Royal Society B*, **280**: 20131224.

CHURCHILL, C.K.C., VALDÉS, Á. & Ó FOIGHIL, D. 2014. Molecular and morphological systematics of neustonic nudibranchs (*Mollusca: Gastropoda: Glaucidae: Glaucus*), with descriptions of three new cryptic species. *Invertebrate Systematics*, **23**: 174–195.

COMEAU, S., GATTUSO, J.P., NISUMAA, A.M. & ORR, J. 2012. Impact of aragonite saturation state changes on migratory pteropods. *Proceedings of the Royal Society B*, **279**: 732–738.

COMEAU, S., JEFFREE, R., TEYSSIÉ, J.L. & GATTUSO, J.P. 2010. Response of the Arctic pteropod *Limacina helicina* to projected future environmental conditions. *PLoS ONE*, **5**: e11362.

CORNILS, A. & HELD, C. 2014. Evidence of cryptic and pseudocryptic speciation in the *Paracalanus parvus* species complex (Crustacea, Copepoda, Calanoida). *Frontiers in Zoology*, **11**: 19.

CORSE, E., RAMPAL, J., CUOC, C., PECH, N., PEREZ, Y. & GILLES, A. 2013. Phylogenetic analysis of Thecosomata Blainville, 1824 (holoplanktonic Opisthobranchia) using morphological and molecular data. *PLoS ONE*, **8**: e59439.

DACOSTA, S., CUNHA, C.M., SIMONE, L.R.L. & SCHRÖDL, M. 2007. Computer-based 3-dimensional reconstruction of major organ systems of a new aeolid nudibranch subspecies, *Flabellina engeli lucianae*, from Brazil (Gastropoda: Opisthobranchia). *Journal of Molluscan Studies*, **73**: 339–353.

DAYRAT, B. & TILLIER, A. 2002. Evolutionary relationships of euthyneuran gastropods (Mollusca): a cladistic re-evaluation of morphological characters. *Zoological Journal of the Linnean Society*, **135**: 403–470.

DAYRAT, B., TILLIER, A., LECOINTRE, G. & TILLIER, S. 2001. New clades of euthyneuran gastropods (Mollusca) from 28S rRNA sequences. *Molecular Phylogenetics and Evolution*, **19**: 225–235.

DONOVAN, D.A., PENNINGS, S.C. & CAREFOOT, T.H. 2006. Swimming in the sea hare *Aplysia brasiliana*: cost of transport, parapodial morphometry, and swimming behavior. *Journal of Experimental Marine Biology and Ecology*, **328**: 76–86.

FAHRNER, A. & HASZPRUNAR, G. 2000. Microanatomy and ultrastructure of the excretory system of two pelagic opisthobranch species (Gastropoda: Gymnosomata and Thecosomata). *Journal of Submicroscopic Cytology and Pathology*, **32**: 185–194.

FEELY, R.A., SABINE, C.L., LEE, W.B., BERELSON, W., KLEYPAS, J., FABRY, V.J. & MILLERO, F.J. 2004. Impact of anthropogenic $CO_2$ on the $CaCO_3$ system in the Oceans. *Science*, **305**: 362.

FRANC, A. 1968. Mollusques gastéropodes et scaphopodes. In: *Traité de Zoologie. Anatomie, Systématique, Biologie*. Vol. 5 (P. Grass, ed.), pp. 608–893. Masson & Cie, Paris.

FRETTER, V. & GRAHAM, A. 1962. *British prosobranch molluscs: their functional anatomy and ecology*. Ray Society, London.

GASCA, R. & JANSSEN, A.W. 2014. Taxonomic review, molecular data and key to the species of Creseidae from the Atlantic Ocean. *Journal of Molluscan Studies*, **80**: 35–42.

GEGENBAUR, C. 1855. *Untersuchungen über Pteropoden und Heteropoden: ein Beitrag zur Anatomie und Entwicklungsgeschichte dieser Thiere*. Verlag Wilhelm Engelmann, Leipzig.

GILMER, R.W. & HARBISON, G.R. 1968. Morphology and field behavior of pteropod molluscs: feeding methods in the families Cavoliniidae, Limacinidae and Peraclididae (Gastropoda: Thecosomata). *Marine Biology*, **91**: 47–57.

GÖBBELER, K. & KLUSSMANN-KOLB, A. 2011. Molecular phylogeny of the Euthyneura (Mollusca, Gastropoda) with special focus on Opisthobranchia as a framework for reconstruction of evolution of diet. *Thalassas*, **27**: 121–154.

HASZPRUNAR, G. 1985. The Heterobranchia—a new concept of the phylogeny of the higher Gastropoda. *Zeitschrift für zoologische Systematik und Evolutionsforschung*, **23**: 15–37.

HASZPRUNAR, G. 1988. On the origin and evolution of major gastropod groups, with special reference to the Streptoneura. *Journal of Molluscan Studies*, **54**: 367–441.

HUBER, G. 1993. On the cerebral nervous system of marine Heterobranchia (Gastropoda). *Journal of Molluscan Studies*, **59**: 381–420.

HUNT, B., STRUGNELL, J., BEDNARŠEK, N., LINSE, K., NELSON, R.J., PAKHOMOV, E., SEIBEL, B., STEINKE, D. & WÜRZBERG, L. 2010. Poles apart: the "bipolar" pteropod species *Limacina helicina* is genetically distinct between the Arctic and Antarctic Oceans. *PLoS ONE*, **5**: e9835.

HUNT, B.P.V., PAKHOMOV, E.A., HOSIE, G.W., SIEGEL, V., WARD, P. & BERNARD, K. 2008. Pteropods in Southern Ocean ecosystems. *Progress in Oceanography*, **78**: 193–221.

JANSSEN, A.W. 2012. Late Quaternary to Recent holoplanktonic Mollusca (Gastropoda) from bottom samples of the eastern Mediterranean Sea: systematics, morphology. *Bollettino Malacologico*, **48**(suppl.): 1–105.

JÖRGER, K.M., NORENBURG, J.L., WILSON, N.G. & SCHRÖDL, M. 2012. Barcoding against a paradox? Combined molecular species delineations reveal multiple cryptic lineages in elusive meiofaunal sea slugs. *BMC Evolutionary Biology*, **12**: 245.

JÖRGER, K.M., STÖGER, I., KANO, Y., FUKUDA, H., KNEBELSBERGER, T. & SCHRÖDL, M. 2010. On the origin of Acochlidia and other enigmatic euthyneuran gastropods, with implications for the systematics of Heterobranchia. *BMC Evolutionary Biology*, **10**: 323.

KLUSSMANN-KOLB, A. 2001. Comparative investigation of the genital systems in the Opisthobranchia (Mollusca, Gastropoda) with special emphasis on the nidamental glandular system. *Zoomorphology*, **120**: 215–235.

KLUSSMANN-KOLB, A., CROLL, R. & STAUBACH, S. 2013. Use of axonal projection patterns for the homologisation of cerebral nerves in Opisthobranchia (Mollusca, Gastropoda). *Frontiers in Zoology*, **10**: 20.

KLUSSMANN-KOLB, A. & DINAPOLI, A. 2006. Systematic position of the pelagic Thecosomata and Gymnosomata within Opisthobranchia (Mollusca, Gastropoda)—revival of the Pteropoda. *Journal of Zoological Systematics and Evolutionary Research*, **44**: 118–129.

KOHNERT, P., BRENZINGER, B., JENSEN, K.R. & SCHRÖDL, M. 2013. 3D-microanatomy of the semiterrestrial slug *Gascoignella aprica* Jensen, 1985—a basal plakobranchacean sacoglossan (Gastropoda, Panpulmonata). *Organisms Diversity & Evolution*, **13**: 583–603.

KOHNERT, P., NEUSSER, T.P., JÖRGER, K.M. & SCHRÖDL, M. 2010. Time for sex change! 3D-reconstruction of the copulatory system

of the 'aphallic' *Hedylopsis ballantinei* (Gastropoda, Acochlidia). *Thalassas*, **27**: 113–119.

KOLLER, K., BRENZINGER, B. & SCHRÖDL, M. 2014. A caenogastropod in 3D: microanatomy of the Munich endemic springsnail *Sadleriana bavarica* Boeters, 1989 (Hydrobiidae). *Spixiana*, **37**: 1–19.

LALLI, C.M. 1970a. Structure and function of the buccal apparatus of *Clione limacina* (Phipps) with a review of feeding in gymnosomatous pteropods. *Journal of Experimental Marine Biology and Ecology*, **4**: 101–118.

LALLI, C.M. 1970b. Morphology of *Crucibranchaea macrochira* (Meisenheimer), a gymnosomatous pteropod. *Journal of Molluscan Studies*, **39**: 1–14.

LALLI, C.M. & GILMER, R.W. 1989. *Pelagic snails: the biology of holoplanktonic gastropod mollusks*. Stanford University Press, Stanford, CA.

LALLI, C.M. & WELLS, F.E. 1978. Reproduction in the genus *Limacina* (Opisthobranchia: Thecosomata). *Journal of Zoology*, **186**: 95–108.

LANGE, R., WERMINGHAUSEN, J. & ANTHES, N. 2013. Does traumatic secretion transfer manipulate mating roles or reproductive output in a hermaphroditic sea slug? *Behavioral Ecology and Sociobiology*, **67**: 1239–1247.

LISCHKA, S. & RIEBESELL, U. 2012. Synergistic effects of ocean acidification and warming on overwintering pteropods in the Arctic. *Global Change Biology*, **18**: 3517–3528.

MAAS, A.E., BLANCO-BERCIAL, L. & LAWSON, G.L. 2013. Reexamination of the species assignment of *Diacavolinia* pteropods using DNA barcoding. *PLoS ONE*, **8**: e53889.

MALAQUIAS, M.A.E., MACKENZIE-DODDS, J., BOUCHET, P., GOSLINER, T. & REID, D.G. 2009. A molecular phylogeny of the Cephalaspidea *sensu lato* (Gastropoda: Euthyneura): Architectibranchia redefined and Runcinacea reinstated. *Zoologica Scripta*, **38**: 23–41.

MEISENHEIMER, J. 1905. Pteropoda. In: *Wissenschaftliche Ergebnisse der Deutschen Tiefsee–Expedition auf dem Dampfer "Valdivia" 1898–1899*. Vol. 9 (C. Chun, ed.), pp. 1–222. G. Fischer, Jena.

NEUSSER, T.P., HEß, M., HASZPRUNAR, G. & SCHRÖDL, M. 2006. Computer-based three-dimensional reconstruction of the anatomy of *Microhedyle remanei* (Marcus, 1953), an interstitial acochlidian gastropod from Bermuda. *Journal of Morphology*, **267**: 231–247.

NEUSSER, T.P., MARTYNOV, A.V. & SCHRÖDL, M. 2009. Heartless and primitive? 3D reconstruction of the polar acochlidian gastropod *Asperspina murmanica*. *Acta Zoologica*, **90**: 228–245.

NEUSSER, T.P. & SCHRÖDL, M. 2007. *Tantulum elegans* reloaded: a computer-based 3D-visualization of the anatomy of a Caribbean freshwater acochlidian gastropod. *Invertebrate Biology*, **126**: 18–39.

ORR, J.C., FABRY, V.J., AUMONT, O., BOPP, L., DONEY, S.C., FEELY, R.A., GNANADESIKAN, A., GRUBER, N., ISHIDA, A., JOOS, F., KEY, R.M., LINDSAY, K., MAIER-REIMER, E., MATEAR, R., MONFRAY, P., MOUCHET, A., NAJJAR, R.G., PLATTNER, G., RODGERS, K.B., SABINE, C.L., SARMIENTO, J.L., SCHLITZER, R., SLATER, R.D., TOTTERDELL, I.J., WEIRIG, M., YAMANAKA, Y. & YOOL, A. 2005. Anthropogenic ocean acidification over the twenty-first century and its impact on calcifying organisms. *Nature*, **437**: 681–686.

RAMPAL, J. 1973. Phylogénie des ptéropodes thécosomes d'après la structure de la coquille et la morphologie du manteau. *Comptes Rendus de l'Académie des Sciences*, *Ser. 2*, **277**: 1345–1348.

RAMPAL, J. 2002. Biodiversité et biogéographie chez les Cavoliniidae (Mollusca, Gastropoda, Opisthobranchia, Euthecosomata). Régions faunistiques marines. *Zoosystema*, **24**: 209–258.

RAMPAL, J. 2011. Clés de determination des ptéropodes thécosomes de Méditerranée et de l'Atlantique euroafricain. *Revue de l'Institut des Pêches Maritimes*, **37**: 369–381.

RANG, M. 1828. Notice sur quelques mollusques nouveaux appartenant au genre *Cleodore* et établissement et monographie du sous-genre *Creseis*. *Annales des Sciences Naturelles*, **13**: 302–319.

RICHARDSON, K.C., JARETT, L. & FINKE, E.H. 1960. Embedding in epoxy resins for ultrathin sectioning in electron microscopy. *Stain Technology*, **35**: 313–323.

ROMEIS, B. 1989. *Mikroskopische Technik*. Urban & Schwarzenberg, München.

RUTHENSTEINER, B. 2008. Soft part 3D visualization by serial sectioning and computer reconstruction. *Zoosymposia*, **1**: 63–100.

SANDERS-ESSER, B. 1984. Vergleichende Untersuchungen zur Anatomie und Histologie der vorderen Genitalorgane der Ascoglossa (Gastropoda, Euthyneura). *Zoologische Jahrbücher*, **111**: 195–243.

SCHMEKEL, L. & PORTMANN, A. 1982. *Opisthobranchia des Mittelmeeres. Nudibranchia und Saccoglossa*. Springer, Berlin.

SCHRÖDL, M., JÖRGER, K., KLUSSMANN-KOLB, A. & WILSON, N.G. 2011. Bye bye "Opisthobranchia"! A review on the contribution of mesopsammic sea slugs to euthyneuran systematics. *Thalassas*, **27**: 101–112.

STAUBACH, S. 2008. The evolution of the cephalic sensory organs within the Opisthobranchia. Dissertation im Fachbereich Biowissenschaften der Johann Wolfgang Goethe—Universität in Frankfurt am Main. p. 155.

STAUBACH, S., SCHÜTZNER, P., CROLL, R.P. & KLUSSMANN-KOLB, A. 2008. Innervation patterns of the cerebral nerves in *Haminoea hydatis* (Gastropoda: Opisthobranchia): a test for intraspecific variability. *Zoomorphology*, **127**: 203–212.

TESCH, J.J. 1913. Mollusca, Pteropoda. In: *Das Tierreich. Eine Zusammenstellung und Kennzeichnung der rezenten Tierformen* (F.E. Schulze, ed.), pp. i–xvi, 1-154.36. Friedberger & Sohn, Berlin.

URIBE, R.A., NAKAMURA, K., INDACOCHEA, A., PACHECO, A.S., HOOKER, Y. & SCHRöDL, M. 2013. A review on the diversity and distribution of opisthobranch gastropods from Peru, with the addition of three new records (Gastropoda, Heterobranchia). *Spixiana*, **36**: 43–60.

VAN DER SPOEL, S. 1967. *Euthecosomata a group with remarkable developmental stages (Gastropoda, Pteropoda)*. J. Noorduijn, Gorinchem, The Netherlands.

WÄGELE, H. & KLUSSMANN-KOLB, A. 2005. Opisthobranchia (Mollusca, Gastropoda)—more than just slimy slugs. Shell reduction and its implications on defence and foraging. *Frontiers in Zoology*, **2**: 1–18.

WÄGELE, H., KLUSSMANN-KOLB, A., VERBEEK, E. & SCHRÖDL, M. 2014. Flashback and foreshadowing – a review of the taxon Opisthobranchia. *Organisms, Diversity & Evolution*, **14**: 133–149.

WÄGELE, H. & WILLAN, R.C. 2000. Phylogeny of the Nudibranchia. *Zoological Journal of the Linnean Society*, **130**: 83–181.

WoRMS. 2014. Euthecosomata. World Register of Marine Species. http://www.marinespecies.org/aphia.php?p=taxdetails&id=23020 (accessed 10 July 2014).